https://doi.org/10.5194/acp-2021-611
Preprint. Discussion started: 6 September 2021

Atmospheric Chemistry and Physics Discussions

Simulated impacts of vertical distributions of black carbon aerosol on meteorology and $PM_{2.5}$ concentrations in Beijing during severe haze events

Donglin Chen[1], Hong Liao[1*], Yang Yang[1], Lei Chen[1], Delong Zhao[2], Deping Ding[2]

[1]Jiangsu Key Laboratory of Atmospheric Environment Monitoring and Pollution Control, Jiangsu Engineering Technology Research Center of Environmental Cleaning Materials, Collaborative Innovation Center of Atmospheric Environment and Equipment Technology, School of Environmental Science and Engineering, Nanjing University of Information Science & Technology, Nanjing, Jiangsu, China

[2]Beijing Weather Modification Office, Beijing 100089, China

*Correspondence to: Hong Liao (hongliao@nuist.edu.cn)

https://doi.org/10.5194/acp-2021-611
Preprint. Discussion started: 6 September 2021

Atmospheric Chemistry and Physics Discussions

Abstract.

Vertical profiles of black carbon (BC) play a critical role in BC-meteorology interaction which influences $PM_{2.5}$ (particulate matter with a diameter of 2.5 μm or less) concentrations. In this study, we used the Weather Research and Forecasting with Chemistry model (WRF-Chem) coupled with an improved integrated process (IPR) analysis scheme to investigate the direct radiative effect (DRE) of BC with different vertical profiles on meteorology and $PM_{2.5}$ concentrations in Beijing during two severe haze events (11-12 December 2016 and 16-19 December 2016). The vertical profiles of BC in Beijing collected by King-Air350 aircraft can be classified into two types: the first type was characterized by decreases in BC concentration with altitude, which was the case mainly controlled by local emissions; the second type had maximum BC concentration around 900 hPa, which was mainly affected by regional transport from the polluted south/southwest region. Compared with measurements in Beijing, the model overestimated BC concentrations by 87.4 % at the surface and underestimated BC mass by 14.9 % at altitudes of 300-900 m altitude as averaged over the two pollution events. The BC DRE with the default vertical profiles from the model heated the air around 300 m altitude but the warming would be stronger when BC vertical profiles were modified for each day using observed data during the two severe haze events. Accordingly, compared to the simulation with the default vertical profiles of BC, planetary boundary layer heights (PBLH) were reduced further by 24.7 m (6.7%) and 6.4 m (3.8%) in Beijing and simulated $PM_{2.5}$ concentrations were higher by 9.3 μg m^{-3} (4.1%) and 5.5 μg m^{-3} (3.0%) over central Beijing in the first and second haze events,

https://doi.org/10.5194/acp-2021-611
Preprint. Discussion started: 6 September 2021


Atmospheric Chemistry and Physics Discussions

respectively, with modified vertical profiles. Furthermore, we quantified by sensitivity experiments the roles of BC vertical profiles with six exponential decline functions ($C(h)=C_0\times e^{-h/hs}$ and hs=0.35, 0.48, 0.53, 0.79, 0.82 and 0.96) parameterized on the basis of the observations and the vertical profile dominated by regional transport. A larger hs leads to a sharper decline of BC concentrations with altitude (less BC at the surface and more BC in the upper atmosphere), resulting in a stronger cooling at the surface (+0.21 with hs of 0.35 vs. -0.13 °C with hs of 0.96) and hence larger reductions in PBLH (larger BC-induced increases in $PM_{2.5}$). Relative to the simulation without BC DRE, the mean $PM_{2.5}$ concentrations were increased by 5.5 μg m^{-3} (3.4%) and 7.9 μg m^{-3} (4.9%) with BC DRE when hs values were 0.35 and 0.96, respectively. Our results indicate that it is very important to have accurate vertical profiles of BC in simulations of meteorology and $PM_{2.5}$ concentrations during haze events.

https://doi.org/10.5194/acp-2021-611
Preprint. Discussion started: 6 September 2021


Atmospheric Chemistry and Physics Discussions

1. Introduction

With the rapid economic development and large increases in fossil energy consumption, haze pollution has become one of the most serious challenges in China, especially in the Beijing-Tianjin-Hebei (BTH) region (Wang et al., 2015; Zhang et al., 2019). In 2014 and 2015, the numbers of extremely serious $PM_{2.5}$ (particulate matter with an aerodynamic equivalent diameter of 2.5 μm or less) pollution days (with daily mean $PM_{2.5}$ > 150 μg m^{-3}) in Beijing reached 45 and 54, respectively (He et al., 2017). The real-time hourly average concentration of $PM_{2.5}$ in Beijing even reached 1000 μg m^{-3} during the severe haze events in January 2013, far exceeding the Chinese Ambient Air Quality Grade I Standards (35 μg m^{-3} for daily mean $PM_{2.5}$) (Liu et al., 2017). With the implementation of the toughest-ever clean air policy since 2013, the observed annual mean $PM_{2.5}$ concentrations averaged over 74 cities in China fell from 61.8 μg m^{-3} in 2013 to 42.0 μg m^{-3} in 2017 (Zhang et al., 2016; Wang et al., 2017a; Li et al., 2019; Zhang et al., 2019). However, severe haze events still occurred in Beijing during the COVID-19 lockdown period (January-February 2020) (Huang et al., 2020; Zhu et al., 2020). Therefore, understanding the mechanisms responsible for the occurrence of severe haze is important for air quality management planning.

BC, an important component of $PM_{2.5}$, is emitted mainly from the incomplete combustion of fossil fuel, biofuel, and biomass burning. BC particles can strongly absorb solar radiation in the atmosphere, which alters the Earth's radiation balance (Bond et al., 2013; Huang et al., 2015; Hu et al., 2020). In recent years, researchers have found that the radiative effect of BC significantly affects the structure of planetary

https://doi.org/10.5194/acp-2021-611
Preprint. Discussion started: 6 September 2021


Atmospheric Chemistry and Physics Discussions

boundary layer (PBL) during severe haze pollution events (Ding et al., 2016; Huang et al., 2018; Wang et al., 2018; Liu et al., 2019). Ding et al. (2016) illustrated by using the Weather Research and Forecasting model coupled with Chemistry (WRF-Chem) that BC suppressed the development of PBL by heating the air in the upper PBL and reducing the solar radiation at the surface in Beijing in December 2013. This process was defined as the "dome effect" of BC by Ding et al. (2016). This "dome effect" was also found over the Indian Ocean (Wilcox et al., 2016). BC can also change the land-sea thermal contrast and induce circulation anomalies during severe haze events (Gao et al., 2016b; Qiu et al., 2017; Ding et al., 2019a; Chen et al., 2021). Ding et al. (2019a) showed by using the WRF-Chem model that, during a haze event in December 2013, the direct radiative effect (DRE) of BC enhanced advection between land and sea by causing a cooling (-1.0 ℃) in air temperature over land and a warming (+0.8 ℃) in air temperature over sea, which transported moist air from the sea to the Yangtze River Delta region. Qiu et al. (2017) and Chen et al. (2021) also reported by using the WRF-Chem model that the radiative effect of BC induced strong anomalous northeasterly winds from the sea during a haze event in North China Plain (NCP) in February 2014.

BC can influence concentrations of $PM_{2.5}$ during haze events because of its impact on PBL and other meteorological fields (Gao et al., 2016b; Wilcox et al., 2016; Miao et al., 2017; Qiu et al., 2017; Gao et al., 2018; Wang et al., 2019; Chen et al., 2021). Gao et al. (2016b) used the WRF-Chem model to simulate the haze event that occurred in the NCP in January 2010 and found a maximum increase in $PM_{2.5}$ of 14.4 μg m^{-3} (5.1%) due to the DRE of BC. Qiu et al. (2017) also analyzed the impact of BC on surface-

https://doi.org/10.5194/acp-2021-611
Preprint. Discussion started: 6 September 2021


Atmospheric Chemistry and Physics Discussions

layer $PM_{2.5}$ during a haze pollution in NCP in February of 2014 by using the WRF-Chem model and found that the average $PM_{2.5}$ concentration increased by 2.1 μg m^{-3} (1.0%) owing to the DRE of BC. Chen et al. (2021) analyzed, by using the WRF-Chem model, the DRE from the aging of BC and its impact on $PM_{2.5}$ concentration over the BTH region during a haze event in February 2014. They found that the near-surface $PM_{2.5}$ concentration average over BTH increased by 9.6 μg m^{-3} (7.0%) due to the aging of BC.

So far few studies examined the impacts of vertical distributions of BC aerosol on meteorology and $PM_{2.5}$ concentrations. Wang et al. (2018) examined the role of BC at different altitudes in influencing PBL height (PBLH) by considering a single column using the WRF-Chem version 3.6.1. They divided the height from 150 to 2250 m evenly into 7 layers and increased BC concentrations from 0 to 30 μg m^{-3} with an increment of 2 μg m^{-3} at one of the layers with the BC concentrations at the other layers fixed to 0 μg m^{-3}. Model results showed that the near-surface BC could increase PBLH by 0% - 4%, while BC aloft would decrease PBLH by 2% - 16% due to the warming of atmosphere by BC. Current chemistry-climate models were reported not to be able to represent the BC vertical profiles accurately, so sensitivity studies were carried out to adjust vertical profiles of BC in the model by changing the vertical resolution, aerosol microphysical scheme and emission height (Wang et al., 2019; Yang et al., 2019; Watson-Parris et al., 2019).

In recent years, measurements of BC vertical distribution have been conducted by aircraft during the severe haze events in Beijing, using a single particle soot photometer

https://doi.org/10.5194/acp-2021-611
Preprint. Discussion started: 6 September 2021


Atmospheric Chemistry and Physics Discussions

(SP2) (Zhao et al., 2018; Tian et al., 2019; Zhao et al., 2019; Tian et al., 2020; Liu et al., 2020). During the period of severe pollution from 11 to 19 December 2016, Zhao et al. (2019) collected BC vertical profiles over Beijing by Air350 aircraft and found that the vertical profiles can be classified into two types. The first type was characterized by decreases in BC concentration with altitude, which was the case mainly controlled by local emissions. The second type had maximum BC concentration around 900 hPa, which was mainly affected by regional transport from the polluted south/southwest region. Generally, the first type occurred more frequently than the second type during haze events in Beijing. Observations of vertical profiles of BC in severe haze events over Beijing in 2018 by a King-Air350 aircraft by Ding et al. (2019b) also obtained the same types of profiles.

In this work, we use the BC vertical profiles observed during two severe haze events (11-12 December 2016 and 16-19 December 2016) over Beijing and the online-coupled WRF-Chem model to investigate the DRE of BC vertical profiles on meteorology and $PM_{2.5}$ concentrations. Compared with previous studies that examined the impact of BC on meteorology and $PM_{2.5}$, our study is the first to pay attention to the role of BC vertical profile as well as the underlying mechanism. The description of the model, observational datasets and numerical experiments are presented in Section 2. Section 3 evaluates simulated meteorological and chemical variables by comparing with observations. Section 4 compares of the DRE of BC with original and modified vertical profiles, and Section 5 discusses the role of BC vertical profiles in influencing meteorological parameters and $PM_{2.5}$ concentrations. The conclusions of this study are

https://doi.org/10.5194/acp-2021-611
Preprint. Discussion started: 6 September 2021


Atmospheric Chemistry and Physics Discussions

given in Section 6.

2. Method

2.1 Model configuration

A fully coupled online Weather Research and Forecasting with Chemistry model (WRF-Chem version 3.7.1) (Grell et al., 2005; Skamarock et al., 2008) was employed to simulate the two severe haze events in Beijing from 7 to 20 December 2016 and the initial 4 days are spin-up. This model adopts Lambert projection and two nested domains with grid resolutions of 30 km (domain 01) and 10 km (domain 02). Figure 1 shows that the outer domain covers the most of China with 100 (west-east) × 100 (south-north) grid cells and the second domain covers the BTH region with 58 (west-east) × 76 (south-north) grid cells. The number of vertical layers is 29 with the first 15 layers below 2 km for finer resolution in the PBL. Meteorological initial and boundary conditions in this model were derived from global reanalysis data (1°×1°) of NCEP (National Center for Environmental Prediction). MOZART-4 (Model for Ozone And Related chemical Tracers-4) simulation results provided the initial and lateral boundary conditions for the concentrations of chemical species in our model (Emmons et al., 2010).

Anthropogenic emission data in year 2016 were obtained from the MEIC inventory with a spatial resolution of 0.25° × 0.25° (Zheng et al., 2018). This inventory includes sulfur dioxide (SO_2), nitrogen oxides (NO_x), carbon monoxide (CO), non-methane volatile organic compounds (NMVOC), ammonia (NH_3), BC, organic carbon (OC),

https://doi.org/10.5194/acp-2021-611
Preprint. Discussion started: 6 September 2021


Atmospheric Chemistry and Physics Discussions

$PM_{2.5}$, PM_{10} and carbon dioxide (CO_2), which were categorized into agriculture, industry, residence, transport and power generation sectors (Li et al., 2015). The biogenic emissions were calculated online using the MEGAN (Model of Emissions of Gases and Aerosol from Nature), including isoprene, terpene and other substances emitted by plants (Guenther et al., 2006). Biomass burning emissions were taken from the Fire Inventory from NCAR (FINN) datasets (Wiedinmyer et al., 2011).

The parameterization schemes of physical and chemical processes of WRF/Chem model adopted in the study are summarized in Table 1. The Carbon-Bond Mechanism version Z (CBMZ) is chosen to simulate the gas-phase chemistry. The aerosols scheme is the Model for Simulating Aerosol Interactions and Chemistry (MOSAIC) which includes sulfate, nitrate, ammonium, chloride, sodium, BC, OC and other inorganic aerosol, and the aerosol particles are divided into 8 particle size segments. However, the formation of secondary organic aerosol is not considered in this scheme (Zhang et al., 2012; Gao et al., 2016a). In MOSAIC, the aerosol particles are assumed to be internal mixture and aerosol optical properties are calculated by the volume averaging mixing method (Barnard et al., 2010; Stelson 1990). The choice for photolysis schemes is Fast-J photolysis scheme.

2.2 Integrated process rate (IPR) analysis

The IPR analysis has been widely applied to illustrate the impacts of each physical/chemical process on the variations in O_3 concentrations (Zhang and Rao, 1999; Jiang et al., 2012; Gao et al., 2017; Gao et al., 2018). The improved IPR analysis method developed by Chen et al. (2019) in WRF-Chem model is used in this work to

https://doi.org/10.5194/acp-2021-611
Preprint. Discussion started: 6 September 2021


Atmospheric Chemistry and Physics Discussions

quantitatively analyze the contributions of physical/chemical processes to $PM_{2.5}$ concentrations, including the contributions from the sub-grid convection (CONV), vertical mixing (VMIX), chemistry (CHEM), regional transport (TRA), wet scavenging (WET), emission source (EMI) and other processes (OTHER). CONV refers to the transport within the sub-grid wet convective updrafts (Chen et al., 2019) and VMIX is affected by atmospheric turbulence and vertical distribution of $PM_{2.5}$ concentrations (Zhang and Rao, 1999; Gao et al., 2018). CHEM represents $PM_{2.5}$ production and loss including gas-phase, cloud and aerosol chemistry. TRA is caused by advection, which is highly related to wind and horizontal distribution of $PM_{2.5}$ concentrations (Gao et al., 2018; Chen et al., 2019). WET represents the wet removal processes of aerosols. EMI is controlled by emission source. OTHER represents the processes other than the above 6 processes in the model. The NET is the sum of all physical and chemical processes, which matches the variations in $PM_{2.5}$ concentrations. It is worth noting that each IPR variable is an accumulated value which is the sum of each time step.

2.3 Observational data

To evaluate the model performance in simulating near-surface meteorological fields, the observed hourly temperature at 2 m (T2), relative humidity at 2 m (RH2), wind speed at 10 m (WS10) and wind direction at 10 m (WD10) at Beijing station are collected from NOAA's National Climatic Data Center (http://gis.ncdc.noaa.gov/maps/ncei/cdo/hourly). The 3-hourly planetary boundary layer (PBL) heights for Beijing were obtained from the Global Data Assimilation System (GDAS) (http://ready.arl.noaa.gov/READYamet.php). The radiosonde data

https://doi.org/10.5194/acp-2021-611
Preprint. Discussion started: 6 September 2021


Atmospheric Chemistry and Physics Discussions

(temperature and relative humidity profiles) in Beijing were obtained from the University of Wyoming, Department of Atmospheric Science (http://weather.uwyo.edu/upperair/sounding.html). Hourly concentrations of $PM_{2.5}$, CO, NO_2, SO_2 and O_3 at Beijing Station were obtained from the China National Environmental Monitoring Center (CNEMC, http://www.cnemc.cn/), which were used to evaluate the model performance in simulating pollutants at the surface. Aerosol optical depth (AOD) at 550 nm over China retrieved from MODIS (Moderate Resolution Imaging Spectroradiometer) satellite was used to evaluate the horizontal distribution of simulated optical properties of aerosols in this study (https://ladsweb.modaps.eosdis.nasa.gov/). The values of daily aerosol optical depth (AOD) at 500 nm and 675 nm in Beijing were obtained from the AERONET data set (https://aeronet.gsfc.nasa.gov/).

The vertical profiles of BC mass concentrations in Beijing were collected by King-Air350 aircraft using SP2 during 11-12 and 16-19 December 2016. The aircraft departured from Shahe (~20 km to the central Beijing) (Fig. 1) at 12:00-13:00 local time (LT) and returned during 15:00-16:00 LT, which avoided the possible diurnal variation of the PBL among flights. Most flights could reach 2.5 km. Zhao et al. (2019) reported that these vertical profiles of BC could be expressed as an exponential decline function $C(h) = C_0 e^{-\frac{h}{hs}}$ except 11 December 2016, where $C(h)$ (μg m^{-3}) is BC concentration at altitude h (km), C_0 (μg m^{-3}) is BC concentration at the surface, and each hs value is calculated for each flight of BC vertical profile using nonlinear regression (Table S1). Tian et al. (2019) observed a regional transport of pollution in

https://doi.org/10.5194/acp-2021-611
Preprint. Discussion started: 6 September 2021


Atmospheric Chemistry and Physics Discussions

Beijing from 10 to 12 December 2016 using SP2 and they found a different vertical structure of BC from that of Zhao et al. (2019), with the BC concentration at the altitudes of 400-900 m being 1.5 times higher than the near-surface BC concentration on 11 December 2016. More detailed information about King-Air350 aircraft dataset can be found in Zhao et al. (2019), Ding et al. (2019b) and Tian et al. (2019).

2.4 Numerical experiments

To compare the DRE of BC with original and corrected vertical profiles and quantify the role of BC vertical profiles in influencing meteorological conditions and air pollutants, we performed the following numerical experiments as summarized in Table 2.

1. CTRL: The control simulation with the direct and indirect radiative effects of all aerosols (BC, OC, sulfate, nitrate, ammonium, Na^+, Cl^- and OIN) included for the time period of 11-20 December 2016. The vertical profiles of BC were the default ones simulated by the model.

2. NoBCrad: The same as the CTRL simulation, except that the DRE of BC was turned off.

3. VerBC_obs: The same as the CTRL simulation, except that the BC vertical profiles in the model were modified according to the observed ones. The specific method will be discussed below.

4. VerBC_hs1-6: The same as the CTRL simulation, except that the vertical profiles of BC in the model were modified according to the exponential decline function ($C(h)=C_0\times e^{-h/hs}$). The values of *hs* in VerBC_hs1 to VerBC_hs6 were 0.35 to 0.96 (from

https://doi.org/10.5194/acp-2021-611
Preprint. Discussion started: 6 September 2021


Atmospheric Chemistry and Physics Discussions

small to large), respectively.

5. VerBC_RT: The same as the VerBC_hs1-6 simulations, except that the BC vertical profiles in the model were modified according to the observed transport BC vertical profile on 11 December 2016 which was affected by regional transport.

In the case of NoBCrad, the BC DRE was turned off by setting the BC mass concentration equal to zero when calculating the optical properties of BC, following the studies of Qiu et al. (2017) and Chen et al. (2021). In VerBC_obs experiment, we modified the simulated BC vertical profile online using the observed BC vertical profile on the corresponding day. Firstly, we interpolated the observed BC concentrations to the height of each layer in the model as $C_{obs\_int(i)}$. Each layer in the model has a top height and a bottom height and we selected the middle height of this layer for interpolation. Secondly, we used $C_{obs\_int(i)}$ to calculate the BC mass column burden in each layer ($M_{obs\_int(i)}$) in the model, and $P_{obs\_int(i)}$ is the percentage of BC mass column burden in each layer to the total BC mass column burden (Fig. S1) calculated by

$$M_{obs\_int(i)} = C_{obs\_int(i)} * (H_{sim\_top(i)} - H_{sim\_bot(i)}) \quad (1)$$

where $H_{sim\_top(i)}$ is the top height of layer i and $H_{sim\_bot(i)}$ is the bottom height of layer i.

$$P_{obs\_int(i)} = \frac{M_{obs\_int(i)}}{\sum_{i=1}^{16} M_{obs\_int(i)}} * 100\% \quad (2)$$

In the VerBC_obs simulation, the simulated BC mass column burden was redistributed to each layer below 2.5 km according to the calculated $P_{obs\_int(i)}$. These procedures ensure that the modification of BC vertical profile for each day in the model by using the observed data does not change the total BC mass column burden. Since the aircraft

https://doi.org/10.5194/acp-2021-611
Preprint. Discussion started: 6 September 2021


Atmospheric Chemistry and Physics Discussions

measured only BC concentrations below 2.5 km, we modify BC profile up to the 16th model layer (about 2.5 km in Beijing).

In the experiment of VerBC_hs1, we also used the above method to modify the BC vertical profile by an exponential decline function which is $C(h)=C_0\times e^{-h/hs}$. However, in cases of VerBC_hs1~6, we modified for the dates of 12 and 16-19 December. On December 11, BC did not show an exponential decline with height due to the regional transport. In simulation of VerBC_RT, the method and setting were the same as VerBC_hs1~6, except that the BC vertical profile in the model was modified according to the observed one on 11 December 2016. In VerBC_obs, VerBC_hs1~6 and VerBC_RT cases, the steps of modifying BC vertical profiles were performed only when the direct radiative forcing of BC was calculated. All other physical and chemical processes still used the original BC vertical profiles simulated by the model.

3 Model evaluation

3.1 Near-surface air pollutants and BC vertical profiles

Figures 2a-2i show the horizontal distributions of simulated near-surface $PM_{2.5}$ concentrations at 2 pm LT from 11 to 19 December 2016. In BTH, high $PM_{2.5}$ concentrations of 138.4 and 90.8 μg m^{-3} occurred on December 11 and 12, respectively. The severe pollution on December 11 was caused by regional transport from the southern heavily polluted area under a prevailing southerly air flow (Tian et al., 2019). From December 16, $PM_{2.5}$ started to accumulate in the eastern China and the concentrations of $PM_{2.5}$ reached highest value of 153.4 μg m^{-3} on 18 December averaged over the BTH region. The daily $PM_{2.5}$ concentrations (Fig. 2j) in Beijing had

https://doi.org/10.5194/acp-2021-611
Preprint. Discussion started: 6 September 2021


Atmospheric Chemistry and Physics Discussions

low values during 13-15 December 2016. The severe pollution during 16-19 December 2016 was mainly affected by local emissions. We are mainly focused on the two heavy pollution incidents (11-12 and 16-19 December 2016) in the following sections.

Results from the CTRL simulation were compared with the observed hourly surface concentrations of $PM_{2.5}$, NO_2, O_3, CO and SO_2 during 11-19 December 2016 in Beijing in Fig. 3. The observed maximum $PM_{2.5}$ concentration of 219.5 μg m^{-3} occurred on December 18, far exceeding the national air quality standard for daily $PM_{2.5}$ of 75 μg m^{-3} (Wang et al., 2017a). The correlation coefficient (R), mean bias (MB), normalized mean bias (NMB) and mean fraction bias (MFB) are summarized in Table 3. The model can reasonably reproduce the temporal variations of $PM_{2.5}$, NO_2, O_3 and CO; the correlation coefficients between simulated and observed hourly concentrations are 0.77, 0.78, 0.66 and 0.73, respectively. The correlation coefficient for SO_2 is lower (0.38). Gao et al. (2016b) explained that WRF-Chem model cannot represent well the SO_2 concentration and its change with time due to the uncertainty in SO_2 emissions and missing heterogeneous oxidation. Compared with observations, the model overestimates the concentrations of $PM_{2.5}$ and NO_2 in Beijing with the MBs and NMBs of (13.2 μg m^{-3}, 10.0%) and (8.5 ppbv, 21.6%), respectively, and underestimates the concentrations of O_3 (-0.1 ppbv, -1.2%) and CO (-0.1 ppmv, -4.9%). Overall, the model can capture the two severe pollution events in Beijing during 11-19 December 2016.

Because of the lack of measured BC vertical profiles from 13-15 December 2016 in Beijing, Figure 4 compares only the simulated vertical profiles of BC with observations for the two polluted events (11-12 and 16-19 December 2016). Observed

https://doi.org/10.5194/acp-2021-611
Preprint. Discussion started: 6 September 2021


Atmospheric Chemistry and Physics Discussions

mass concentrations of BC decreased exponentially with altitude in all days except for December 11 when regional transport of pollution dominated. On December 11, the observed maximum mass concentration of BC (7.0 μg m^{-3}) occurred at 850 m altitude, which was much higher than the surface-layer concentration of 4.7 μg m^{-3}. Compared with the observed vertical profiles of BC, the model can well represent the decreases of BC mass concentration with height on December 12 and 16-19, but cannot reproduce the vertical profile on December 11. Averaged over the two pollution events, the simulated BC mass concentration was overestimated by 87.4% on the ground and underestimated by 33.1% at altitude of 1000 m compared with the observations in Beijing. The inaccuracy of the vertical distribution of BC would lead to inaccurate representation of the interactions between BC and PBL, especially in heavily polluted events.

3.2 Meteorological parameters

On December 12-16 and 18-19, Beijing was mainly controlled by northerlies and northwesterlies, which transported clean air mass to Beijing. On December 11 and 17, southwesterlies brought polluted air to Beijing, as shown in Fig. 2. Nevertheless, the average wind speed in Beijing was 5.1 m s^{-1} at 850 hPa on December 17, which was much smaller than 11.0 m s^{-1} at 850 hPa on December 11, which explains that Beijing was less affected by the regional pollution transport on December 17. Figure 5 shows the hourly simulated and observed T2, RH2, WS10, WD10 and PBLH in Beijing from 11 to 19 December 2016. The statistical metrics are summarized in Table 3. In the two severe haze events, the observed maximum RH2 in each day exceeded 70.0%, which

https://doi.org/10.5194/acp-2021-611
Preprint. Discussion started: 6 September 2021


Atmospheric Chemistry and Physics Discussions

accelerated the formation of secondary aerosols (Sun et al., 2006; Wang et al., 2014). Compared with the observations, the model can well represent the temporal variation of T2 and RH2 with correlation coefficients of 0.77 and 0.75, respectively, but slightly overestimates T2 with a MB of 0.1 ℃ and underestimates RH2 with a MB of 3.4%. For WS10, observations and simulated results both show low wind speed with the mean values of 1.5 and 1.4 m s^{-1} in Beijing during the two periods of haze events. Such meteorological condition was very beneficial to the accumulation of near-surface pollution. The WRF-Chem model also captures the high values of WS10 from 14 to 15 December. For wind direction at 10 m, the NMB is -9.0% and the R is 0.45, which indicates that the model can simulate the change of wind direction during the period of heavy pollution. For PBL, the observed PBL was 118.7 m during the two severe haze events, compared to 287.5 m during the clean period. The model can represent the change of PBLH in Beijing from 11 to 19 December 2016 with R of 0.72. However, the model overestimates the PBLH by 30.9 m (17.7%) in Beijing averaged over 11-19 December 2016.

The simulated and observed vertical profiles of temperature in Beijing during 11-19 December 2016 are shown in Fig. S2. The observed temperature vertical profiles are available only at 8:00 and 20:00. During the two severe pollution events, strong temperature inversions below 1500 m were observed in Beijing, which inhibited vertical mixing and caused the accumulation of pollutants near the ground. The model captures these temperature inversions well but overestimates the inversion layer height on December 11 and underestimates the inversion layer height from 16 to 19 December.

https://doi.org/10.5194/acp-2021-611
Preprint. Discussion started: 6 September 2021


Atmospheric Chemistry and Physics Discussions

The inaccuracy of the simulated inversion layer height may be due to the fact that the model cannot correctly represent the vertical profiles of BC (Fig. 4).

3.3 AOD and AAOD

AOD (AAOD) is the measure of aerosols (absorbing aerosols) distributed within a column of air from the surface to the top of the atmosphere (Khor et al., 2014). Figure S3 shows the horizontal spatial distributions of observed and simulated AOD at 550 nm over the NCP averaged over 11-19 December 2016. The model can well simulate the horizontal distribution of AOD, with a spatial correlation coefficient of 0.89. However, the model underestimates AOD over the NCP region. Many previous studies have shown that MODIS retrieval tends to overestimate AOD over NCP (Li et al., 2016; Qiu et al., 2017). We also compared the simulated hourly AAOD at 550 nm with AERONET AAOD in Beijing and Xianghe station in Fig. 6. The correlation coefficient between simulations and observations is 0.85. Compared with AERONET AAOD, simulated AAOD values at Beijing and Xianghe are overestimated by 0.02 (33.3%) and 0.02 (39.9%), respectively.

4. A comparison of BC DRE with original and modified vertical profiles

As shown in Fig. 4, the model does not represent well the vertical distribution of BC concentrations during the two heavily polluted events, especially on December 11. So, in this section, we examine the differences in the BC DRE on meteorology and concentrations of pollutants with the original and modified vertical profiles.

4.1 Direct radiative effect of BC on meteorology

https://doi.org/10.5194/acp-2021-611
Preprint. Discussion started: 6 September 2021


Atmospheric Chemistry and Physics Discussions

383 Figure 7 shows the atmospheric temperature and PBLH simulated from the CTRL
384 simulation and their changes caused by BC DRE with original profiles (CTRL minus
385 NoBCrad) and modified profiles (VerBC_obs minus NoBCrad), over Beijing from 11
386 to 19 December 2016. Light-absorbing BC heated the air at around 300 m on December
387 11 and 16-19, regardless of the original or modified BC vertical profiles (Fig. 7b and
388 7c). With the original and modified BC profiles, the maximum warming effects in the
389 PBL were 0.8 ℃ and 0.9 ℃, respectively, at 14:00 LT on December 18. Although BC
390 concentration was the highest at the surface, the largest increase in temperature
391 occurred in the upper layers because of the stronger shortwave absorption efficiency of
392 BC at higher altitude (Ding et al., 2016; Wang et al., 2018). The warming at around 300
393 m resulted in a more stable stratification, thereby weakening convective motions (Gao
394 et al., 2018). The largest reductions in PBLH were 133.8 m (28.0%) at 14:00 LT on
395 December 12 and 141.2 m (59.0%) at 14:00 LT on December 18 in Beijing with original
396 and modified BC vertical profiles, respectively. On December 11 when regional
397 transport of pollution dominated, relative to the simulation with original BC profile,
398 simulated air temperature with modified profile was lower by about 0.5 ℃ within the
399 PBL (Fig. 7d), which was caused by the observed maximum mass concentration of BC
400 around 850 m altitude (Fig. 4a). Correspondingly, the maximum reduction in PBLH of
401 74.2 m was also simulated on December 11. On December 16-19 when local emissions
402 dominated, compared the effects of original BC profiles, the air temperatures at around
403 300 m were all higher with modified BC. The largest difference of +0.1 ℃ was
404 simulated in the PBL on December 18 (Fig. 7d).

https://doi.org/10.5194/acp-2021-611
Preprint. Discussion started: 6 September 2021


Atmospheric Chemistry and Physics Discussions

405 The spatial distribution of 10-m winds averaged over the two severe haze events is
406 shown in Fig. S4. When the BC DRE was not considered in NoBCrad simulation, the
407 overall wind speed in Beijing was weak with a mean value of 3.6 m s^{-1}, which made it
408 difficult for local emissions to diffuse. The westerlies in the central part of NCP brought
409 relatively clean air to Beijing. Compared to the baseline of NoBCrad, the BC DRE with
410 original and modified vertical profiles both enhanced the northerlies north of NCP and
411 weakened the wind speed in central and southern Beijing.

412 **4.2 Direct radiative effect of BC on $PM_{2.5}$ concentration**

413 By altering the meteorological conditions, BC exerts feedback onto $PM_{2.5}$
414 concentrations. Figure 8 shows the spatial distributions of changes in near-surface
415 $PM_{2.5}$ induced by BC DRE with original (CTRL minus NoBCrad, Figs. 8a1-8a2) and
416 modified (VerBC_obs minus NoBCrad, Figs. 8b1-8b2) vertical profiles, as well as the
417 differences between VerBC_obs and CTRL (VerBC_obs minus CTRL, Figs. 8c1-8c2)
418 over Beijing in the two haze events. Because of the differences in BC-induced changes
419 in air temperature, wind field, and PBLH, changes in near-surface $PM_{2.5}$ concentrations
420 in the northern and southern Beijing were different. In the first haze event of 11-12
421 December, although PBLH was reduced in the northern Beijing due to BC DRE,
422 enhanced northerlies brought in relatively clean air to northern Beijing, leading to
423 decreases in near-surface $PM_{2.5}$ concentrations with maximum values of 12.5 μg m^{-3}
424 (9.4%) and 10.6 μg m^{-3} (8.0%) in this region with the original and modified BC vertical
425 profiles, respectively. Nevertheless, $PM_{2.5}$ concentrations increased by up to 17.8 μg m^{-3}
426 (6.6%) and 24.0 μg m^{-3} (9.3%) in the southern Beijing due to BC effect with original

https://doi.org/10.5194/acp-2021-611
Preprint. Discussion started: 6 September 2021


Atmospheric Chemistry and Physics Discussions

and modified vertical profiles, respectively. In the second haze event of 16-19 December, the near-surface $PM_{2.5}$ concentrations increased in most areas of Beijing with both vertical profiles. Compared to the simulation with the original profiles, the modified profiles of BC led to larger increases in $PM_{2.5}$ concentrations over Beijing, and the maximum differences in $PM_{2.5}$ were simulated over central Beijing, which were 9.3 μg m^{-3} (3.6%) and 5.5 μg m^{-3} (3.1%) in the first and second haze events, respectively.

To explain the changes in near-surface $PM_{2.5}$ concentrations in Beijing due to BC effects, we carried out process analysis for $PM_{2.5}$ for 12:00-18:00 of each day when the DRE of BC is the largest (Figs. 8a3, 8b3, and 8c3). From 11 to 19 December 2016, VMIX had dominant positive contribution to changes in $PM_{2.5}$ concentration, which reached the maximum contributions of 32.4 μg m^{-3} and 33.9 μg m^{-3} on December 18 with original and modified BC vertical profiles, respectively. The vertical mixing was strongly restrained by PBLH, therefore, the decreases in PBLH caused accumulation of $PM_{2.5}$ in the lower layers. Meanwhile, CHEM contributed 4.8 μg m^{-3} and 6.1 μg m^{-3} to $PM_{2.5}$ changes because more aerosol precursors restrained in the boundary layer led to the formation of secondary particles. TRA was the major process that had negative contribution to the changes in $PM_{2.5}$, which can be explained by the enhanced northerlies in the central part of NCP due to BC effects as shown in Fig S4. Relative to the case with original BC vertical profiles, VMIX and CHEM contributions increased largely with modified profiles, with increases of 8.6 μg m^{-3} (6.5%) and 7.7 μg m^{-3} (26.8%), respectively, as averaged over the two haze events, reflecting the further decreases in PBLH (Fig. 7d).

https://doi.org/10.5194/acp-2021-611
Preprint. Discussion started: 6 September 2021


Atmospheric Chemistry and Physics Discussions

Figure 9 shows the vertical profiles of the contributions of physical/chemical processes to changes in $PM_{2.5}$ over Beijing due to BC DRE with original (CTRL minus NoBCrad; Figs. 9a1 and 9b1) and modified vertical profiles (VerBC_obs minus NoBCrad; Figs. 9a2 and 9b2) in the two haze events. In the first haze event of 11-12 December when regional transport of pollution dominated, the NET contribution to $PM_{2.5}$ was positive below 256 m, because of the positive contribution of VMIX was larger than the negative contribution of TRA. However, in the upper layers (from 256 to 1555 m), the contributions of VMIX and CHEM became negative with both original and modified vertical profiles, which can be explained by the decreases in PBLH inhibiting the transport of low-layer pollutants to the upper layer. Compared to the original BC vertical profiles, the modified BC vertical profiles increased $PM_{2.5}$ in the entire vertical layers below 2080 m, in which the positive contribution between 256-757 m was caused by TRA. These results agree with the observed high concentrations of BC at altitudes of 600-1500 m on December 11 (Fig. 4a). In the second haze event, the NET contribution to $PM_{2.5}$ was positive below 127 m and negative at 127-504 m. However, the effects of BC on $PM_{2.5}$ were small above 504 m because BC concentrations decreased rapidly with altitude.

5. Roles of BC vertical profiles

BC has higher light-absorbing efficiency at higher altitudes (Ding et al., 2016; Wang et al., 2018). As described in Section 2.3, the observed vertical profiles of BC on heavily polluted days (12 and 16-19 December) can be parameterized as exponential decline functions using nonlinear regression ($C(h)=C_0\times e^{-h/hs}$) with *hs* values of 0.35,

https://doi.org/10.5194/acp-2021-611
Preprint. Discussion started: 6 September 2021


Atmospheric Chemistry and Physics Discussions

0.48, 0.53, 0.79, 0.82 and 0.96, and the profiles affected by regional transport had high concentrations of BC at high altitudes. We conducted seven sensitivity experiments which applied six exponential functions and one observed transport-dominated vertical profile, as described in Section 2.4, to examine the roles of BC vertical profiles in influencing meteorological conditions and $PM_{2.5}$ during severe haze events. In these sensitivity experiments, we only modify the BC vertical profiles for the dates of 12 and 16-19 December. In the function of $C(h)=C_0\times e^{-h/hs}$, a larger *hs* leads to a sharper decline of BC concentrations with altitude (less BC at the surface and more BC in the upper atmosphere), as shown in Fig. 10.

5.1 Impacts of BC vertical profiles on meteorology

Figure 11 shows the simulated changes in atmospheric temperature induced by BC DRE with exponential functions (VerBC_hs1-6 minus NoBCrad) and with the transport-dominated vertical profile (VerBC_RT minus NoBCrad). BC had a significant warming effect at altitudes of 256-421 m from 12:00 to 18:00 (Fig. 7). Generally, with the value of *hs* gradually increasing, the BC-induced warming in the afternoon around 300 m became smaller, which can be explained by the highest mass fraction of BC at the altitudes of 256-421 m to total BC column burden in VerBC_hs1 case (31.7%) and the lowest percentage in VerBC_hs6 case (21.7%) among the six sensitivity experiments (Fig. S1). The maximum warming around 300 m was 0.42 ℃ in VerBC_hs1 case and 0.19 ℃ in VerBC_hs6 case. It should be noted that BC led to a significant cooling effect at the surface (below 80 m) when *hs* values were 0.79, 0.82 and 0.96, with the changes in temperature by -0.08, -0.09 and -0.13 ℃, respectively.

https://doi.org/10.5194/acp-2021-611
Preprint. Discussion started: 6 September 2021


Atmospheric Chemistry and Physics Discussions

493 Because more BC mass was assigned into high altitudes (above 1000 m) with higher
494 *hs*, less solar radiation could reach the ground (Fig. S5). These results are consistent
495 with those found in previous modeling and observational studies (Cappa et al., 2012;
496 Ferrero et al., 2014; Ding et al., 2016; Wang et al., 2018). Meanwhile, in the case of
497 VerBC_RT, BC also had a cooling effect of 0.30 ℃ at the surface (Fig. 11g). Many
498 studies could hardly simulate the cooling of BC at the surface, which might be caused
499 by the vertical profiles of BC in the model (Wang et al., 2019).

500 We further use the difference in temperature between the upper PBL (T_H; 256-421
501 m) and the ground (T_L; 0-127 m) ($\Delta T_{BC} = T_H - T_L$) averaged over 12:00-18:00 LT of 12
502 and 16-19 December to quantify temperature inversion caused by BC DRE. With *hs*
503 values increasing from 0.35 to 0.96, ΔT_{BC} increased from 0.17 to 0.42 ℃, and the ΔT_{BC}
504 value was 0.51 ℃ in VerBC_RT case (Fig. 12a). As a result, the reductions in PBLH
505 were larger with higher *hs* (Fig. 12b). The minimum decrease in PBLH was -31.9 m (-
506 14.3%) with *hs* value of 0.35 and the maximum decrease was 48.9 m (22.0%) with *hs*
507 value of 0.96, as averaged the period of 12:00-18:00 of 12, 16-19 December. In the case
508 of VerBC_RT, the mean PBLH was reduced by 56.9 m (25.6%) during the period of
509 12:00–18:00.

510 ## 5.2 Impacts of BC vertical profiles on $PM_{2.5}$ concentration

511 Figure 13a shows the changes in surface-layer $PM_{2.5}$ concentration caused by BC
512 DRE with six exponential functions (VerBC_hs1-6 minus NoBCrad) and the transport-
513 dominated vertical profile (VerBC_RT minus NoBCrad) averaged over 12 December
514 and 16-19 December 2016. From 0:00 to 11:00, the surface-layer $PM_{2.5}$ exhibited larger

https://doi.org/10.5194/acp-2021-611
Preprint. Discussion started: 6 September 2021


Atmospheric Chemistry and Physics Discussions

BC-induced decreases with a higher value of *hs*. This can be explained by the negative contribution of TRA process that increased during the period of 0:00-5:00 (Figs. 13b and 13c) when *hs* value changed from 0.35 to 0.96. The near-surface $PM_{2.5}$ concentration was reduced by up to 9.1 μg m^{-3} (6.2%) and 12.6 μg m^{-3} (8.6%) at 5:00 with *hs* values of 0.35 and 0.96, respectively. Compared to the NoBCrad case, the surface-layer $PM_{2.5}$ concentrations were reduced by up to 13.8 μg m^{-3} (9.4%) at 5:00 due to BC DRE in VerBC_RT case. From 12:00 to 18:00, the BC-induced increases in surface-layer $PM_{2.5}$ concentrations were larger as *hs* values are higher; relative to NoBCrad simulation, the mean $PM_{2.5}$ concentrations were increased by 5.5 μg m^{-3} (3.4%) and 7.9 μg m^{-3} (4.9%) with the *hs* values of 0.35 and 0.96, respectively. Because the PBL was suppressed by BC DRE from 12:00 to 15:00, the contributions of VMIX and CHEM to near-surface $PM_{2.5}$ were positive and larger in magnitude than the negative contribution of TRA. The NET of all processes was negative from 16:00 to 18:00 due to the continuous growth of negative contribution of TRA. The negative contribution of TRA process from 12:00 to 18:00 can be explained by the enhanced northerlies in the central part of BTH caused by BC DRE, which transported cleaner air mass into Beijing (Fig S6). From 19:00 to 23:00, the surface-layer $PM_{2.5}$ concentrations were decreased by BC DRE, which can be explained by the dominant negative contribution of TRA from 19:00 to 21:00. At 22:00, the reduction in surface-layer $PM_{2.5}$ was 7.5 μg m^{-3} (4.0%) when hs value was 0.35 and 6.6 μg m^{-3} (3.5%) when *hs* was 0.96.

6. Conclusions

https://doi.org/10.5194/acp-2021-611
Preprint. Discussion started: 6 September 2021


Atmospheric Chemistry and Physics Discussions

537 In this study, a fully coupled online WRF-Chem model with an improved integrated
538 process rate (IPR) analysis scheme is employed to investigate the direct radiative effects
539 (DRE) of BC vertical profiles on meteorology and $PM_{2.5}$ concentrations during two
540 severe haze events (11-12 December 2016 and 16-19 December 2016). Compared to
541 the vertical profiles of BC in Beijing collected by King- Air350 aircraft using SP2, the
542 default vertical profiles of BC from the WRF-Chem model can capture the decreases
543 of BC mass concentration with altitude on December 12 and 16-19 when local
544 emissions dominated, but cannot reproduce the observed maximum mass concentration
545 of BC around 850-m altitude on December 11 when regional transport of pollutants
546 dominated. Averaged over the two severe pollution events, the model overestimates BC
547 mass concentration by 87.4% at the surface but underestimates BC by 33.1% at 1000-
548 m altitude compared with the observations in Beijing.

549 We carried out simulations with both the default original BC vertical profiles and
550 the modified vertical profiles using the observations (keep the column burden of BC
551 from the WRF-Chem but distribute BC mass vertically according to the observed
552 fractions of BC in individual model layers for each day). Compared with the simulation
553 with original BC profiles, the warming by BC DRE around 300-m altitude was stronger
554 with the modified profiles. Accordingly, the BC-induced reductions in PBLH in Beijing
555 averaged over the two severe haze events were 43.4 m (18.4%) and 55.4 m (23.5%),
556 respectively, with the original and modified profiles. As a result, relative to the
557 simulation with the original profiles, the modified profiles of BC led to larger increases
558 in $PM_{2.5}$ concentrations by BC DRE. The maximum differences in $PM_{2.5}$ (VerBC_obs

https://doi.org/10.5194/acp-2021-611
Preprint. Discussion started: 6 September 2021


Atmospheric Chemistry and Physics Discussions

559 minus CTRL) were simulated over central Beijing, which were 9.3 μg m^{-3} (4.1%) and
560 5.5 μg m^{-3} (3.0%) in the first and second haze events, respectively. IPR analysis is used
561 to explain the changes in $PM_{2.5}$ concentrations caused by BC DRE. During the two
562 severe haze events, VMIX and CHEM had the dominant positive contributions to the
563 changes in surface-layer $PM_{2.5}$ due to the reductions in PBLH, and TRA had the key
564 negative contribution to $PM_{2.5}$ changes.

565 Seven sensitivity experiments were further carried out to understand the roles of
566 BC vertical profiles. In six assumed exponential functions ($C(h)=C_0\times e^{-h/hs}$) with *hs*
567 values of 0.35, 0.48, 0.53, 0.79, 0.82 and 0.96, a larger *hs* leads to a sharper decline of
568 BC concentrations with altitude (less BC at the surface and more BC in the upper
569 atmosphere). In all the cases, the simulated largest warming occurred at altitudes of
570 256-421 m. With the value of *hs* gradually increasing, the BC-induced warming in the
571 afternoon around 300-m altitude became smaller, the maximum warming was 0.42 ℃
572 in VerBC_hs1 case (*hs*=0.35) and the minimum warming was 0.19 ℃ in VerBC_hs6
573 case (*hs*=0.96). While BC led to warming of 0.21, 0.08 and 0.04 ℃ at the surface when
574 *hs* values were 0.35, 0.48 and 0.53, it led to a significant cooling near the surface (below
575 80 m) when *hs* values were 0.79, 0.82 and 0.96, with the changes in temperature by -
576 0.08, -0.09 and -0.13 ℃, respectively. Stronger temperature inversion with higher *hs*
577 led to larger BC-induced increases in $PM_{2.5}$; relative to NoBCrad simulation, the mean
578 $PM_{2.5}$ concentrations were increased by 5.5 μg m^{-3} (3.4%) and 7.9 μg m^{-3} (4.9%) with
579 the *hs* values of 0.35 and 0.96, respectively.

580 Results from our study highlight the importance of accurate representation of BC

https://doi.org/10.5194/acp-2021-611
Preprint. Discussion started: 6 September 2021


Atmospheric Chemistry and Physics Discussions

vertical profiles in models, which alter the radiation balance, BC-PBL interaction, and hence the simulated $PM_{2.5}$ concentrations. Due to the limitation of observational data, this study was focused on the DRE of BC vertical profiles on meteorology and $PM_{2.5}$ concentration in Beijing during severe haze events. However, the results from this study should be generally important for understanding severe haze for urban areas.

There are channels for further improvement in near-future research. We distribute BC mass vertically according to the observed fractions of BC in individual model layers for each day without considering the hourly variations of BC vertical profiles due to the lack of data. Such assumed distribution of BC based on observation may not be consistent with the dynamic processes (winds, temperature, etc.) of the atmosphere. Further efforts are needed to examine the roles of BC vertical profiles in coupled chemistry-weather models.

https://doi.org/10.5194/acp-2021-611
Preprint. Discussion started: 6 September 2021

Atmospheric Chemistry and Physics Discussions

Data availability.

The WRF-Chem model is available at https://www2.mmm.ucar.edu/wrf/users/downloads.html (last access: 7 July 2020). The observations and simulation results are available upon request from the corresponding author (hongliao@nuist.edu.cn).

Competing interests.

The authors declare that they have no conflict of interest.

Author contributions.

DC and HL designed the study and DC wrote the paper. DC performed model simulations and analyzed the data. DZ and DD provided the observed data. YY and LC provided technical support.

Acknowledgements.

This work was supported by the National Key Research and Development Program of China (grant no. 2019YFA0606804), the National Natural Science Foundation of China (grant no. 42021004), and the Major Research Plan of the National Social Science Foundation (grant no.18ZDA052).

https://doi.org/10.5194/acp-2021-611
Preprint. Discussion started: 6 September 2021

Atmospheric Chemistry and Physics Discussions

References

Barnard, J. C., Fast, J. D., Paredesmiranda, G., Arnott, W. P., and Laskin, A.: Technical Note: Evaluation of the WRF-Chem "Aerosol Chemical to Aerosol Optical Properties" Module using data from the MILAGRO campaign, Atmos. Chem. Phys., 10, 7325-7340, https://doi.org/10.5194/acp-10-7325-2010, 2010.

Bond, T. C., Doherty, S. J., Fahey, D. W., Forster, P. M., Berntsen, T., Deangelo, B., Flanner, M. G., Ghan, S. J., Karcher, B., and Koch, D.: Bounding the role of black carbon in the climate system: A scientific assessment, J. Geophys. Res.-Atmos., 118, 5380-5552, https://doi.org/10.1002/jgrd.50171, 2013.

Cappa, C.D., Onasch, T.B., Massoli, P., Worsnop, D.R., Bates, T.S., Cross, E.S., Davidovits, P., Hakala, J., Hayden, K.L., Jobson, B.T., Kolesar, K.R., Lack, D.A., Lerner, B.M., Li, S.-M., Mellon, D., Nuaaman, I., Olfert, J.S., Petäjä, T., Quinn, P.K., Song, C., Subramanian, R., Williams, E.J., Zaveri, R.A.: Radiative absorption enhancements due to the mixing state of atmospheric black carbon, Science, 337, 1078–1081, https://doi.org/10.1126/science.1223447, 2012.

Chen, D., Liao, H., Yang, Y., Chen, L., and Wang, H.: Simulated aging processes of black carbon and its impact during a severe winter haze event in the Beijing-Tianjin-Hebei region, Sci. Total Environ., 755, p.142712, https://doi.org/10.1016/j.scitotenv.2020.142712, 2021.

Chen, L., Zhu, J., Liao, H., Gao, Y., Qiu, Y., Zhang, M., Liu, Z., Li, N., and Wang, Y.: Assessing the formation and evolution mechanisms of severe haze pollution in the Beijing–Tianjin–Hebei region using process analysis, Atmos. Chem. Phys., 19, 10845-10864, https://doi.org/10.5194/acp-19-10845-2019, 2019.

Ding, A. J., Huang, X., Nie,W., Sun, J. N., Kerminen, V. M., Petäjä, T., Su, H., Cheng, Y. F., Yang, X. Q., Wang, M. H., Chi, X. G., Wang, J. P., Virkkula, A., Guo, W. D., Yuan, J., Wang, S. Y., Zhang, R. J., Wu, Y. F., Song, Y., Zhu, T., Zilitinkevich, S., Kulmala, M., and Fu, C. B.: Enhanced haze pollution by black carbon in megacities in China, Geophys. Res. Lett., 43, 2873–2879, https://doi.org/10.1002/2016gl067745, 2016.

https://doi.org/10.5194/acp-2021-611
Preprint. Discussion started: 6 September 2021


Atmospheric Chemistry and Physics Discussions

644 Ding, Q., Sun, J., Huang, X., Ding, A., Zou, J., Yang, X., and Fu, C.: Impacts of black
645 carbon on the formation of advection–radiation fog during a haze pollution episode
646 in eastern China, Atmos. Chem. Phys., 19, 7759-7774,
647 https://doi.org/10.5194/acp-19-7759-2019, 2019a.
648 Ding, S., Liu, D., Zhao, D., Hu, K., Tian, P., Zhou, W., Huang, M., Yang, Y., Wang, F.,
649 and Sheng, J.: Size-Related Physical Properties of Black Carbon in the Lower
650 Atmosphere over Beijing and Europe, Environ. Sci. Technol., 53, 11112-11121,
651 https://doi.org/10.1021/acs.est.9b03722, 2019b.
652 Emmons, L. K., Walters, S., Hess, P. G., Lamarque, J., Pfister, G., Fillmore, D., Granier,
653 C., Guenther, A., Kinnison, D. E., and Laepple, T.: Description and evaluation of
654 the Model for Ozone and Related chemical Tracers, version 4 (MOZART-4),
655 Geosci. Model Dev., 3(1), 43-67, https://doi.org/10.5194/gmd-3-43-2010, 2010.
656 Ferrero, L., Castelli, M., Ferrini, B., Moscatelli, M., Perrone, M., Sangiorgi, G.,
657 Dangelo, L., Rovelli, G., Moroni, B., Scardazza, F.: Impact of black carbon aerosol
658 over Italian basin valleys: high-resolution measurements along vertical profiles,
659 radiative forcing and heating rate, Atmos. Chem. Phys., 14, 9641–9664,
660 https://doi.org/10.5194/acp-14-9641-2014, 2014.
661 Gao, J., Zhu, B., Xiao, H., Kang, H., Hou, X., Yin, Y., Zhang, L., and Miao, Q.: Diurnal
662 variations and source apportionment of ozone at the summit of Mount Huang, a
663 rural site in Eastern China, Environ. Pollut., 222, 513–522,
664 https://doi.org/10.1016/j.envpol.2016.11.031, 2017.
665 Gao, J., Zhu, B., Xiao, H., Kang, H., Pan, C., Wang, D., and Wang, H.: Effects of black
666 carbon and boundary layer interaction on surface ozone in Nanjing, China, Atmos.
667 Chem. Phys., 18, 7081-7094, https://doi.org/10.5194/acp-18-7081-2018, 2018.
668 Gao, M., Carmichael, G. R., Wang, Y., Ji, D., Liu, Z., and Wang, Z.: Improving
669 simulations of sulfate aerosols during winter haze over Northern China: the
670 impacts of heterogeneous oxidation by NO_2, Front. Environ. Sci. Technol., 10(5),
671 1-11, https://doi.org/10.1007/s11783-016-0878-2, 2016a.
672 Gao, M., Carmichael, G. R., Wang, Y., Saide, P. E., Yu, M., Xin, J., Liu, Z., and Wang,
673 Z.: Modeling study of the 2010 regional haze event in the North China Plain,

https://doi.org/10.5194/acp-2021-611
Preprint. Discussion started: 6 September 2021

Atmos. Chem. Phys., 16, 1673-1691, https://doi.org/10.5194/acp-16-1673-2016, 2016b.

Grell, G. A., Peckham, S. E., Schmitz, R., Mckeen, S. A., Frost, G. J., Skamarock, W. C., and Eder, B.: Fully coupled "online" chemistry within the WRF model, Atmos. Environ., 39, 6957-6975, https://doi.org/10.1016/j.atmosenv.2005.04.027, 2005.

Guenther, A., Karl, T., Harley, P., Wiedinmyer, C., Palmer, P. I. and Geron, C.: Estimates of global terrestrial isoprene emissions using MEGAN (Model of Emissions of Gases and Aerosols from Nature), Atmos. Chem. Phys., 6(11), 3181–3210, https://doi.org/10.5194/acp-6-3181-2006, 2006.

He, J., Gong, S., Yu, Y., Yu, L., Wu, L., Mao, H., Song, C., Zhao, S., Liu, H., and Li, X.: Air pollution characteristics and their relation to meteorological conditions during 2014–2015 in major Chinese cities, Environ. Pollut., 223, 484-496, https://doi.org/ 10.1016/j.envpol.2017.01.050, 2017.

Hong, S., Noh, Y., and Dudhia, J.: A New Vertical Diffusion Package with an Explicit Treatment of Entrainment Processes, Mon. Weather Rev., 134, 2318-2341, https://doi.org/10.1175/MWR3199.1, 2006.

Hu, K., Zhao, D., Liu, D., Ding, S., Tian, P., Yu, C., Zhou, W., Huang, M., and Ding, D.: Estimating radiative impacts of black carbon associated with mixing state in the lower atmosphere over the northern North China Plain, Chemosphere, 252, https://doi.org/10.1016/j.chemosphere.2020.126455, 2020.

Huang, X., Ding, A., Gao, J., Zheng, B., Zhou, D., Qi, X., Tang, R., Wang, J., Ren, C., Nie, W., Chi, X., Xu, Z., Chen, L., Li, Y., Che, F., Pang, N., Wang, H., Tong, D., Qin, W., Cheng, W., Liu, W., Fu, Q., Liu, B., Chai, F., Davis, S. J., Zhang, Q., and He, K.: Enhanced secondary pollution offset reduction of primary emissions during COVID-19 lockdown in China, Natl. Sci. Rev., nwaa137, https://doi.org/10.31223/OSF.IO/HVUZY, 2020.

Huang, X., Song, Y., Zhao, C., Cai, X., Zhang, H., and Zhu, T.: Direct Radiative Effect by Multicomponent Aerosol over China, J. Climate, 28, 3472-3495, https://doi.org/10.1175/JCLI-D-14-00365.1, 2015.

Huang, X., Wang, Z., and Ding, A.: Impact of Aerosol-PBL Interaction on Haze

https://doi.org/10.5194/acp-2021-611
Preprint. Discussion started: 6 September 2021


Atmospheric Chemistry and Physics Discussions

Pollution: Multiyear Observational Evidences in North China, Geophys. Res. Lett., 45, 8596-8603, https://doi.org/10.1029/2018GL079239, 2018.

Jiang, F., Zhou, P., Liu, Q., Wang, T., Zhuang, B., and Wang, X.: Modeling tropospheric ozone formation over East China in springtime, J. Atmos. Chem., 69(4), 303-319, https://doi.org/10.1007/s10874-012-9244-3, 2012.

Khor, W. Y., Hee, W. S., Tan, F., San Lim, H., Jafri, M. Z. M., and Holben, B.: Comparison of Aerosol optical depth (AOD) derived from AERONET sunphotometer and Lidar system, IOP Conf. Ser.: Earth Environ. Sci., 20, https://doi.org/10.1088/1755-1315/20/1/012058, 2014.

Li, K., Jacob, D. J., Liao, H., Zhu, J., Shah, V., Shen, L., Bates, K. H., Zhang, Q., and Zhai, S.: A two-pollutant strategy for improving ozone and particulate air quality in China, Nat. Geosci., 12, 906-910, https://doi.org/10.1038/s41561-019-0464-x, 2019.

Li, K., Liao, H., Zhu, J., and Moch, J. M.: Implications of RCP emissions on future $PM_{2.5}$ air quality and direct radiative forcing over China, J. Geophys. Res.-Atmos., 121, https://doi.org/10.1002/2016JD025623, 2016.

Li, M., Zhang, Q., Kurokawa, J., Woo, J., He, K. B., Lu, Z., Ohara, T., Song, Y., Streets, D. G., and Carmichael, G. R.: MIX: a mosaic Asian anthropogenic emission inventory for the MICS-Asia and the HTAP projects, Atmos. Chem. Phys., 15, 34813-34869, https://doi.org/10.5194/acpd-15-34813-2015, 2015.

Liu, D., Zhao, D., Xie, Z., Yu, C., Chen, Y., Tian, P., Ding, S., Hu, K., Lowe, D., Liu, Q., Zhou, W., Wang, F., Sheng, J., Kong, S., Hu, D., Wang, Z., Huang, M., and Ding, D.: Enhanced heating rate of black carbon above the planetary boundary layer over megacities in summertime, Environ, Res, Lett., 14, https://doi.org/10.1088/1748-9326/ab4872, 2019.

Liu, Q., Liu, D., Gao, Q., Tian, P., Wang, F., Zhao, D., Bi, K., Wu, Y., Ding, S., and Hu, K.: Vertical characteristics of aerosol hygroscopicity and impacts on optical properties over the North China Plain during winter, Atmos. Chem. Phys., 1-34, https://doi.org/10.5194/acp-20-3931-2020, 2020.

Liu, T., Gong, S., He, J., Yu, M., Wang, Q., Li, H., Liu, W., Zhang, J., Li, L., Wang, X.,

https://doi.org/10.5194/acp-2021-611
Preprint. Discussion started: 6 September 2021

734 Zhang, J., Li, L., Wang, X., Li, S., Lu, Y., Du, H., Wang, Y., Zhou, C., Liu, H., and
735 Zhao, Q.: Attributions of meteorological and emission factors to the 2015 winter
736 severe haze pollution episodes in China's Jing-Jin-Ji area, Atmos. Chem. Phys., 17,
737 2971-2980, https://doi.org/10.5194/acp-17-2971-2017, 2017.
738 Miao, Y., Guo, J., Liu, S., Liu, H., Li, Z., Zhang, W., and Zhai, P.: Classification of
739 summertime synoptic patterns in Beijing and their associations with boundary
740 layer structure affecting aerosol pollution, Atmos. Chem. Phys., 17, 3097-3110,
741 https://doi.org/10.5194/acp-17-3097-2017, 2017.
742 Qiu, Y., Liao, H., Zhang, R., and Hu, J.: Simulated impacts of direct radiative effects of
743 scattering and absorbing aerosols on surface layer aerosol concentrations in China
744 during a heavily polluted event in February 2014, J. Geophys. Res.-Atmos., 122,
745 5955-5975, https://doi.org/10.1002/2016JD026309, 2017.
746 Skamarock, W. C., Klemp, J. B., Dudhia, J., Gill, D. O., Barker, D. M., Wang, W., and
747 Powers, J. G.: A description of the advanced research WRF version 2, NCAR Tech.
748 Note, NCAR/TN-468CSTR, Natl. Cent. Atmos. Res., Boulder, Colo, available at:
749 http://wrf-model.org/wrfadmin/publications.php (last access: 6 August 2020),
750 2008.
751 Stelson, A. W.: Urban aerosol refractive index prediction by partial molar refraction
752 approach, Environ. Sci. Technol., 24, 1676-1679,
753 https://doi.org/10.1021/es00081a008, 1990.
754 Sun, Y., Zhuang, G., Tang, A., Wang, Y., and An, Z.: Chemical Characteristics of $PM_{2.5}$
755 and PM_{10} in Haze−Fog Episodes in Beijing, Environ. Sci. Technol., 40, 3148-3155,
756 https://doi.org/10.1021/es051533g, 2006.
757 Tian, P., Liu, D., Huang, M., Liu, Q., Zhao, D., Ran, L., Deng, Z. Z., Wu, Y., Fu, S., and
758 Bi, K.: The evolution of an aerosol event observed from aircraft in Beijing: An
759 insight into regional pollution transport, Atmos. Environ., 206, 11-20,
760 https://doi.org/10.1016/j.atmosenv.2019.02.005, 2019.
761 Tian, P., Liu, D., Zhao, D., Yu, C., Liu, Q., Huang, M., Deng, Z., Ran, L., Wu, Y., and
762 Ding, S.: In situ vertical characteristics of optical properties and heating rates of
763 aerosol over Beijing, Atmos. Chem. Phys., 20(4), 2603-2622,

https://doi.org/10.5194/acp-2021-611
Preprint. Discussion started: 6 September 2021


Atmospheric Chemistry and Physics Discussions

https://doi.org/10.5194/acp-20-2603-2020, 2020.

Wang, H., Xue, M., Zhang, X., Liu, H., Zhou, C., Tan, S., Che, H., Chen, B., and Li, T.: Mesoscale modeling study of the interactions between aerosols and PBL meteorology during a haze episode in Jing–Jin–Ji (China) and its nearby surrounding region–Part 1: Aerosol distributions and meteorological features, Atmos. Chem. Phys., 15, 3257-3275, https://doi.org/10.5194/acp-15-3277-2015, 2015.

Wang, J., Zhao, B., Wang, S., Yang, F., Xing, J., Morawska, L., Ding, A., Kulmala, M., Kerminen, V., Kujansuu, J., Wang, Z., Ding, D., Zhang, X., Wang, H., Tian, M., Petäjä, T., Jiang, J., and Hao, J.: Particulate matter pollution over China and the effects of control policies, Sci. Total Environ., 584, 426-447, https://doi.org/10.1016/j.scitotenv.2017.01.027, 2017a.

Wang, Y., Ying, Q., Hu, J., and Zhang, H.: Spatial and temporal variations of six criteria air pollutants in 31 provincial capital cities in China during 2013-2014, Environ. Int., 73, 413-422, https://doi.org/10.1016/j.envint.2014.08.016, 2014.

Wang, Z., Huang, X., and Ding, A.: Dome effect of black carbon and its key influencing factors: a one-dimensional modelling study, Atmos. Chem. Phys., 18, 2821-2834, https://doi.org/10.5194/acp-18-2821-2018, 2018.

Wang, Z., Huang, X., and Ding, A.: Optimization of vertical grid setting for air quality modelling in China considering the effect of aerosol-boundary layer interaction, Atmos. Environ., 210, 1-13, https://doi.org/10.1016/j.atmosenv.2019.04.042, 2019.

Watsonparris, D., Schutgens, N., Reddington, C. L., Pringle, K. J., Liu, D., Allan, J. D., Coe, H., Carslaw, K. S., and Stier, P.: In situ constraints on the vertical distribution of global aerosol, Atmos. Chem. Phys., 19, 11765-11790, https://doi.org/10.5194/acp-19-11765-2019, 2019.

Wiedinmyer, C., Akagi, S. K., Yokelson, R. J., Emmons, L. K., Alsaadi, J. A., Orlando, J. J., and Soja, A. J.: The Fire INventory from NCAR (FINN): a high resolution global model to estimate the emissions from open burning, Geosci. Model Dev., 4, 625-641, https://doi.org/10.5194/gmd-4-625-2011, 2011.

https://doi.org/10.5194/acp-2021-611
Preprint. Discussion started: 6 September 2021

794 Wilcox, E. M., Thomas, R., Praveen, P. S., Pistone, K., Bender, F. A. M., and
795 Ramanathan, V.: Black carbon solar absorption suppresses turbulence in the
796 atmospheric boundary layer, Proc. Natl. Acad. Sci. USA, 113, 11794-11799,
797 https://doi.org/10.1073/pnas.1525746113, 2016.
798 Wild, O., Zhu, X., and Prather, M. J.: Fast-J: Accurate Simulation of In- and Below-
799 Cloud Photolysis in Tropospheric Chemical Models, J. Atmos. Chem., 37, 245-
800 282, https://doi.org/10.1023/A:1006415919030, 2000.
801 Yang, Y., Smith, S., Wang, H., Lou, S., and Rasch, P.: Impact of Anthropogenic
802 Emission Injection Height Uncertainty on Global Sulfur Dioxide and Aerosol
803 Distribution, J. Geophys. Res.-Atmos., 124, 4812-4826,
804 https://doi.org/10.1029/2018JD030001, 2019.
805 Zaveri, R. A., and Peters, L. K.: A new lumped structure photochemical mechanism for
806 large-scale applications, J. Geophys. Res.-Atmos., 104, 30387-30415,
807 https://doi.org/10.1029/1999JD900876, 1999.
808 Zaveri, R. A., Easter, R. C., Fast, J. D., and Peters, L. K.: Model for Simulating Aerosol
809 Interactions and Chemistry (MOSAIC), J. Geophys. Res., 113, -,
810 https://doi.org/10.1029/2007JD008782, 2008.
811 Zhang, H., Wang, S., Hao, J., Wang, X., Wang, S., Chai, F., and Li, M.: Air pollution
812 and control action in Beijing, J. Clean. Prod., 112, 1519-1527,
813 https://doi.org/10.1016/j.jclepro.2015.04.092, 2016.
814 Zhang, J., and Rao, S. T.: The Role of Vertical Mixing in the Temporal Evolution of
815 Ground-Level Ozone Concentrations, J. Appl. Meteorol., 38, 1674-1691,
816 https://doi.org/10.1175/1520-0450(1999)038<1674:TROVMI>2.0.CO;2, 1999.
817 Zhang, Q., Zheng, Y., Tong, D., Shao, M., Wang, S., Zhang, Y., Xu, X., Wang, J., He,
818 H., Liu, W., Ding, Y., Lei, Y., Li, J., Wang, Z., Zhang, X., Wang, Y., Cheng, J., Liu,
819 Y., Shi, Q., Yan, L., Geng, G., Hong, C., Li, M., Liu, F., Zheng, B., Cao, J., Fu, Q.,
820 Huo, J., Liu, B., Liu, Z., Yang, F., He, K., and Hao, J.: Drivers of improved $PM_{2.5}$
821 air quality in China from 2013 to 2017, Proc. Natl. Acad. Sci. USA, 116, 24463-
822 24469, https://doi.org/10.1073/pnas.1907956116, 2019.
823 Zhang, Y., Chen, Y., Sarwar, G., and Schere, K.: Impact of gas-phase mechanisms on

https://doi.org/10.5194/acp-2021-611
Preprint. Discussion started: 6 September 2021

824 Weather Research Forecasting Model with Chemistry (WRF/Chem) predictions:
825 Mechanism implementation and comparative evaluation, J. Geophys. Res.-Atmos.,
826 117, https://doi.org/10.1029/2011JD015775, 2012.
827 Zhao, C., Liu, X., Ruby Leung, L., and Hagos, S.: Radiative impact of mineral dust on
828 monsoon precipitation variability over West Africa, Atmos. Chem. Phys., 11,
829 1879–1893, https://doi.org/10.5194/acp-11-1879-2011, 2011.
830 Zhao, D., Huang, M., Liu, D., Ding, D., Tian, P., Liu, Q., Zhou, W., Sheng, J., Wang,
831 F., Bi, K., Yang, Y., Li, X., Hu, Y., Guo, X., Gao, Y., He, H., Chen, Y., Kong, S.,
832 and Huang, J.: Aircraft measurements of black carbon in the boundary layer over
833 the North China Plain, Atmos. Chem. Phys., 1-25, https://doi.org/10.5194/acp-
834 2017-1118, 2018.
835 Zhao, D., Huang, M., Tian, P., He, H., Lowe, D., Zhou, W., Sheng, J., Wang, F., Bi, K.,
836 Kong, S., Yang, Y., Liu, Q., Liu, D., and Ding, D.: Vertical characteristics of black
837 carbon physical properties over Beijing region in warm and cold seasons, Atmos.
838 Environ., 213, 296-310, https://doi.org/10.1016/j.atmosenv.2019.06.007, 2019.
839 Zheng, B., Tong, D., Li, M., Liu, F., Hong, C., Geng, G., Li, H., Li, X., Peng, L., Qi, J.,
840 Yan, L., Zhang, Y., Zhao, H., Zheng, Y., He, K., and Zhang, Q.: Trends in China's
841 anthropogenic emissions since 2010 as the consequence of clean air actions,
842 Atmos. Chem. Phys., 18, 14095-14111, https://doi.org/10.5194/acp-18-14095-
843 2018, 2018.
844 Zhu, J., Chen, L., Liao, H., Yang, H., Yang, Y., and Yue, X.: Enhanced $PM_{2.5}$ Decreases
845 and O_3 Increases in China during COVID-19 Lockdown by Aerosol-Radiation
846 Feedback, Geophys. Res. Lett., 48(2), https://doi.org/10.1029/2020GL090260,
847 2020.
848

https://doi.org/10.5194/acp-2021-611
Preprint. Discussion started: 6 September 2021

Atmospheric Chemistry and Physics Discussions

849 **Table1.** Physical and chemical options for WRF/Chem.

WRF/Chem Model Configuration	Description
Microphysics scheme	Lin microphysics scheme (Wiedinmyer et al., 2011)
Longwave radiation scheme	RRTMG scheme (Zhao et al., 2011)
Shortwave radiation scheme	RRTMG scheme (Zhao et al., 2011)
Gas phase chemistry scheme	CBMZ (Zaveri and Peters, 1999)
Aerosol module	MOSAIC (Zaveri et al., 2008)
Photolysis scheme	Fast-J (Wild et al., 2000)
Boundary layer scheme	Yonsei University Scheme(YSU) (Hong et al., 2006)
Pavement parameterization scheme	Noah Land Surface Model scheme

850

851

https://doi.org/10.5194/acp-2021-611
Preprint. Discussion started: 6 September 2021

Atmospheric Chemistry and Physics Discussions

852 **Table 2.** Numerical experiments. Y indicates "on", and N indicates "off".

Simulations	BC direct radiative effect (DRE)		
	DRE	BC vertical profiles for calculation of DRE	
	Turn on/off	Types description	Modified dates
CTRL	Y	Simulated by model	No modification
NoBCrad	N	Simulated by model	No modification
VerBC_obs	Y	Modified according to intraday observations	11-12 and 16-19 December
VerBC_hs1-6	Y	Modified according to $C(h)=C_0\times e^{-h/hs}$ function[a]	12 and 16-19 December
VerBC_RT	Y	Modified according to observations on 11 December 2016	12 and 16-19 December

853 [a] The values of *hs* in VerBC_hs1, VerBC_hs2, VerBC_hs3, VerBC_hs4, VerBC_hs5 and

854 VerBC_hs6 are 0.35, 0.48, 0.53, 0.79, 0.82 and 0.96, respectively.

855

https://doi.org/10.5194/acp-2021-611
Preprint. Discussion started: 6 September 2021

Atmospheric Chemistry and Physics Discussions

Table 3. Statistical metrics for temperature at 2 m (T2; ℃), relative humidity at 2 m (RH2; %), wind speed at 10 m (WS10; m s^{-1}), wind direction at 10 m (WD10, °), $PM_{2.5}$ (μg m^{-3}), SO_2 (ppbv), NO_2 (ppbv), CO (ppmv) and O_3 (ppbv).

Variables	SIM[a]	OBS[b]	R[c]	MB[d]	NMB[e]	MFB[f]
T2 (℃)	-0.5	-0.6	0.77	0.1	-17.8	-13.1
RH2 (%)	52.5	55.8	0.75	-3.4	-6.0	-0.3
WS10 (m s^{-1})	1.8	2.3	0.52	-0.5	-20.6	-11.5
WD10 (°)	165.6	182.0	0.45	-16.4	-9.0	0.7
PBLH (m)	205.8	174.9	0.72	30.9	17.7	72.9
$PM_{2.5}$ (μg m^{-3})	145.6	132.3	0.77	13.2	10.0	15.7
SO_2 (ppbv)	7.9	7.8	0.38	0.1	0.0	-2.9
NO_2 (ppbv)	47.7	39.2	0.78	8.5	21.6	20.2
CO (ppmv)	1.8	1.9	0.73	-0.1	-4.9	6.4
O_3 (ppbv)	6.7	6.8	0.66	-0.1	-1.2	-36.0

[a,b] SIM and OBS represent the averaged model results and observations in Beijing from 11 to 19 December 2016.

[c] R is the correlation coefficient which is calculated between hourly observations and simulations in Beijing from 11 to 19 December 2016, $R = \frac{\sum_{i=1}^{n}|(OBS_i-OBS)*(SIM_i-SIM)|}{\sqrt{\sum_{i=1}^{n}(OBS_i-OBS)^2+\sum_{i=1}^{n}(SIM_i-SIM)^2}}$, where OBS_i and SIM_i are the hourly observed and simulated data in Beijing and n is the total number of hours.

[d] MB is the mean bias, $MB = \frac{1}{n}*\sum_{i=1}^{n} SIM_i - OBS_i$.

[e] NMB is the normalized mean bias, $NMB = \frac{1}{n}*\sum_{i=1}^{n}\frac{SIM_i-OBS_i}{OBS_i}*100\%$.

[f] MFB is the mean fraction bias, $MFB = \frac{2}{n}*\sum_{i=1}^{n}\frac{SIM_i-OBS_i}{SIM_i+OBS_i}*100\%$.

https://doi.org/10.5194/acp-2021-611
Preprint. Discussion started: 6 September 2021

Atmospheric Chemistry and Physics Discussions

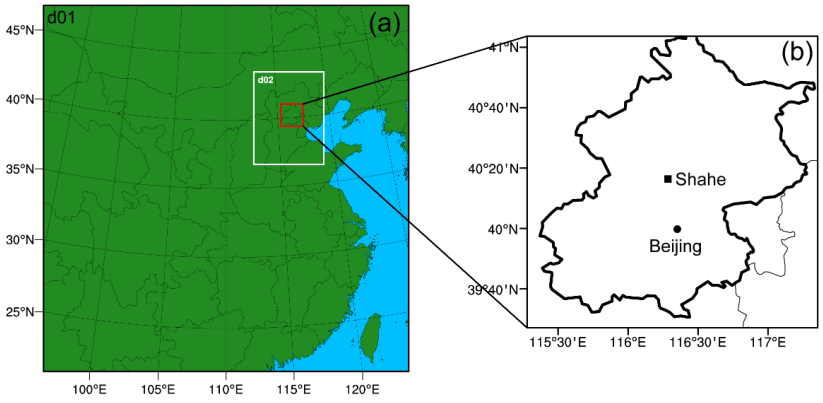

868

869 **Figure 1.** (a) Two nested domains with grid resolutions of 30 km (d01) and 10 km (d02).

870 (b) The BC vertical profiles were modified for the red box which covers the whole of

871 Beijing.

872

https://doi.org/10.5194/acp-2021-611
Preprint. Discussion started: 6 September 2021

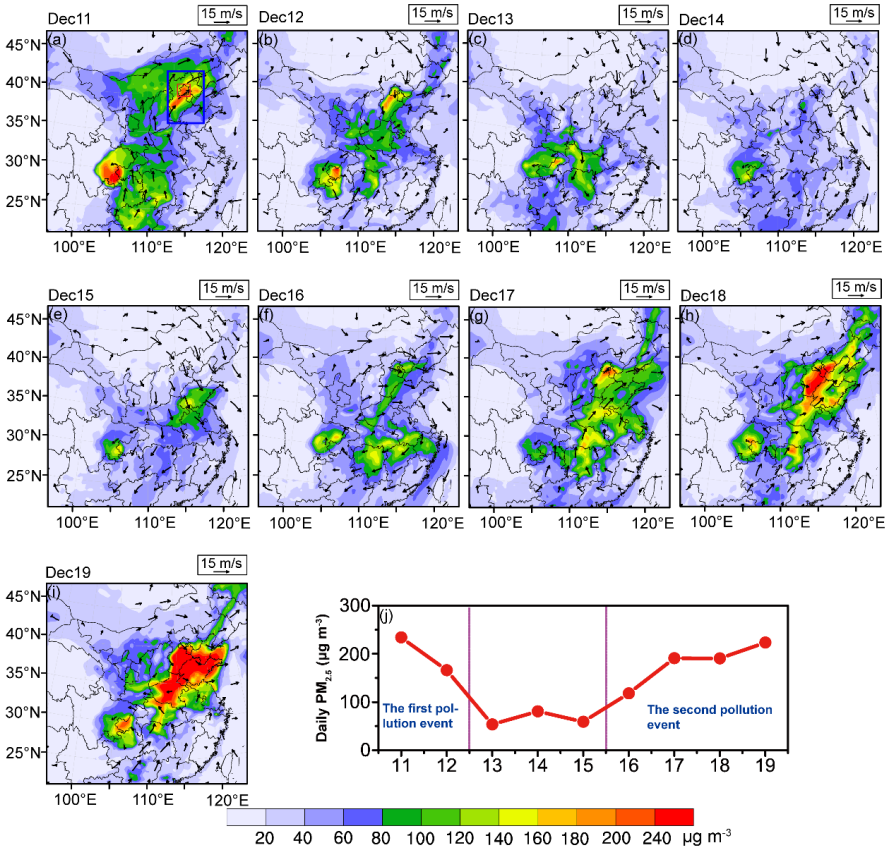

Figure 2. (a-i) Simulated spatial distributions of $PM_{2.5}$ concentrations (μg m^{-3}) and winds (m s^{-1}) at 850 hPa at 2 pm local time from 11 to 19 December 2016. (j) Time series of simulated daily $PM_{2.5}$ concentration in Beijing from 11 to 19 December 2016. Blue and red squares in the first panel denote the Beijing-Tianjin-Hebei and Beijing region, respectively.

https://doi.org/10.5194/acp-2021-611
Preprint. Discussion started: 6 September 2021

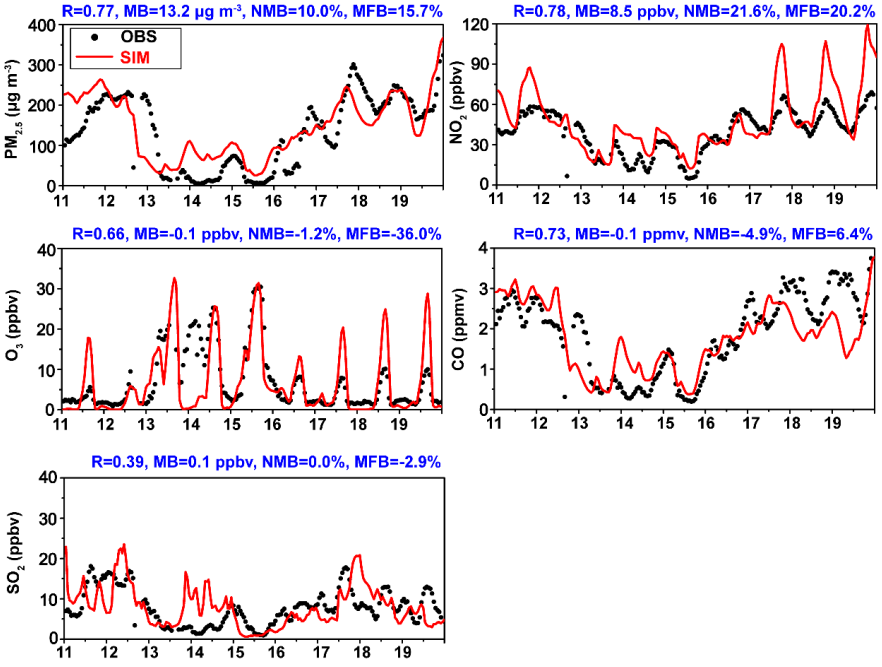

Figure 3. Time series of the observed (black dots) and simulated (red lines) hourly concentrations of $PM_{2.5}$ (μg m^{-3}), NO_2 (ppbv), O_3 (ppbv), CO (ppmv), SO_2 (ppbv) and BC (μg m^{-3}) in Beijing from 11 to 19 December 2016.

https://doi.org/10.5194/acp-2021-611
Preprint. Discussion started: 6 September 2021

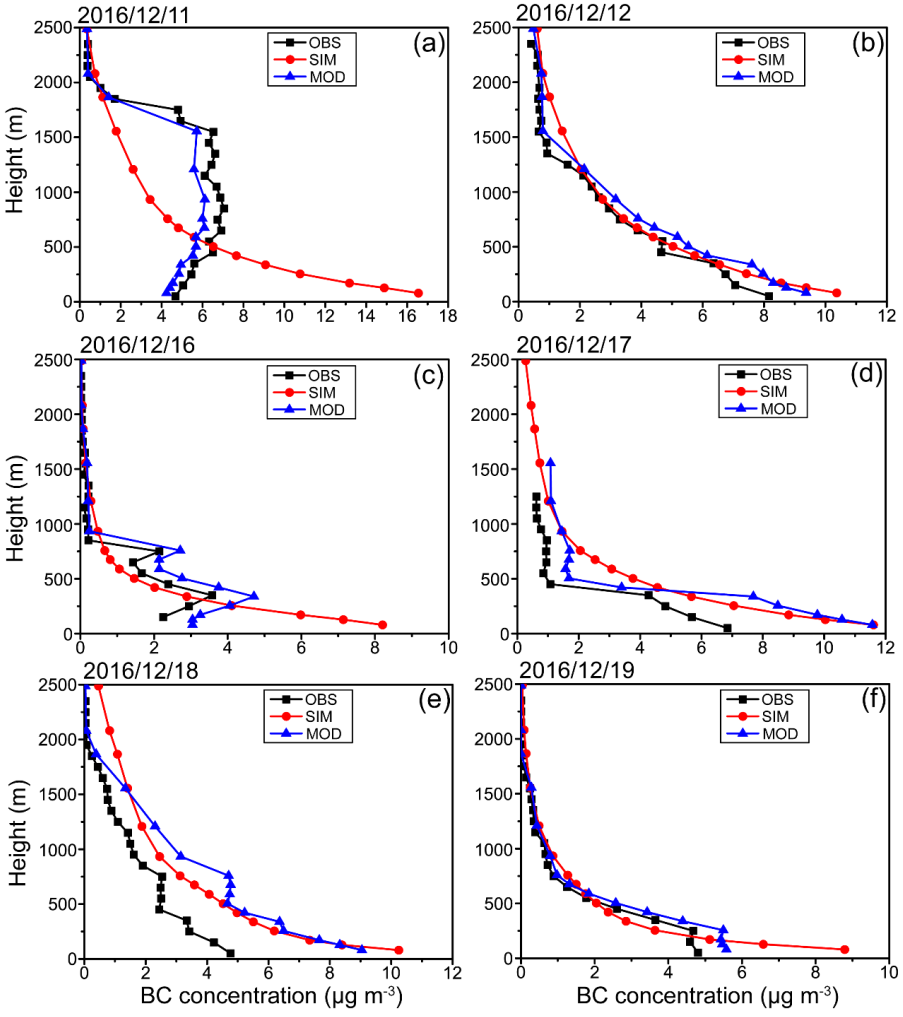

Figure 4. Observed (black line), simulated (red line) and modified (blue line) BC vertical profiles in Beijing on 11-12 and 16-19 December 2016.

https://doi.org/10.5194/acp-2021-611
Preprint. Discussion started: 6 September 2021

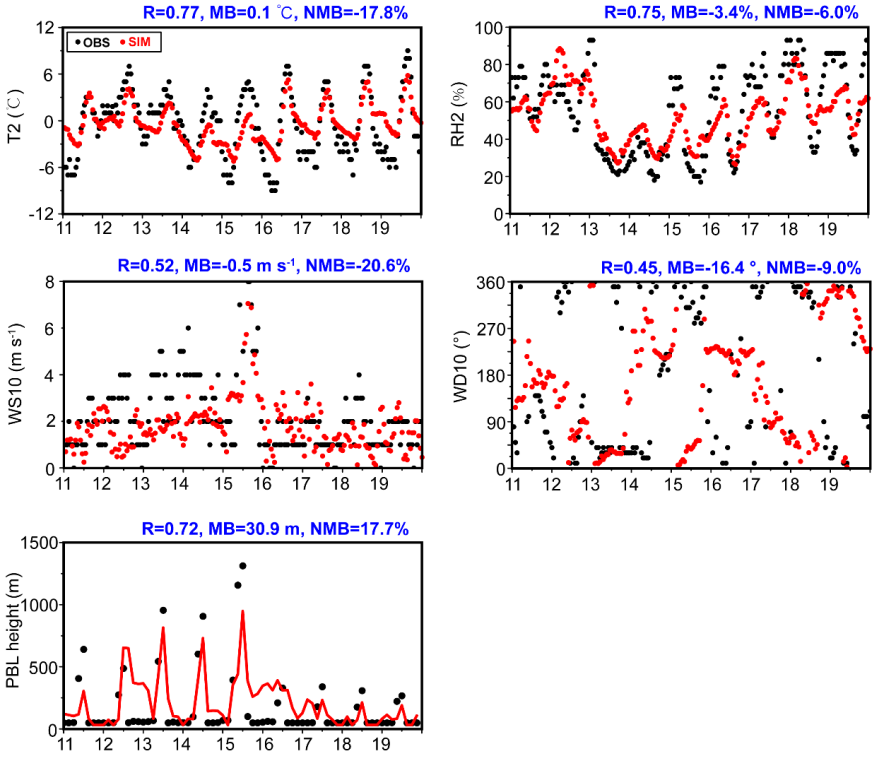

Figure 5. The black and red dots are the observed and simulated data of T2 (℃), RH2 (%), PBL height (m), WS10 (m s^{-1}) and WD10 (°) in Beijing from 11 December 2016 to 19 December 2016.

https://doi.org/10.5194/acp-2021-611
Preprint. Discussion started: 6 September 2021

Atmospheric Chemistry and Physics Discussions

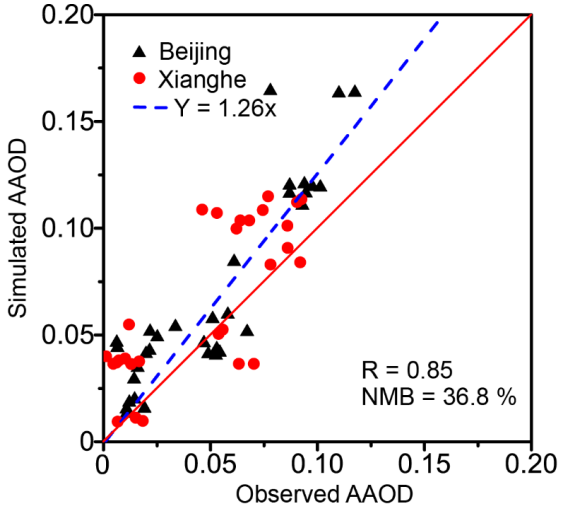

894

895 **Figure 6.** Comparison of simulated absorption aerosol optical depth (AAOD) at 550
896 nm with observations in Beijing (116.38°E, 39.98°N) and Xianghe (116.96°E, 39.75°N)
897 station from 11 to 19 December 2016.

898

https://doi.org/10.5194/acp-2021-611
Preprint. Discussion started: 6 September 2021

Atmospheric Chemistry and Physics Discussions

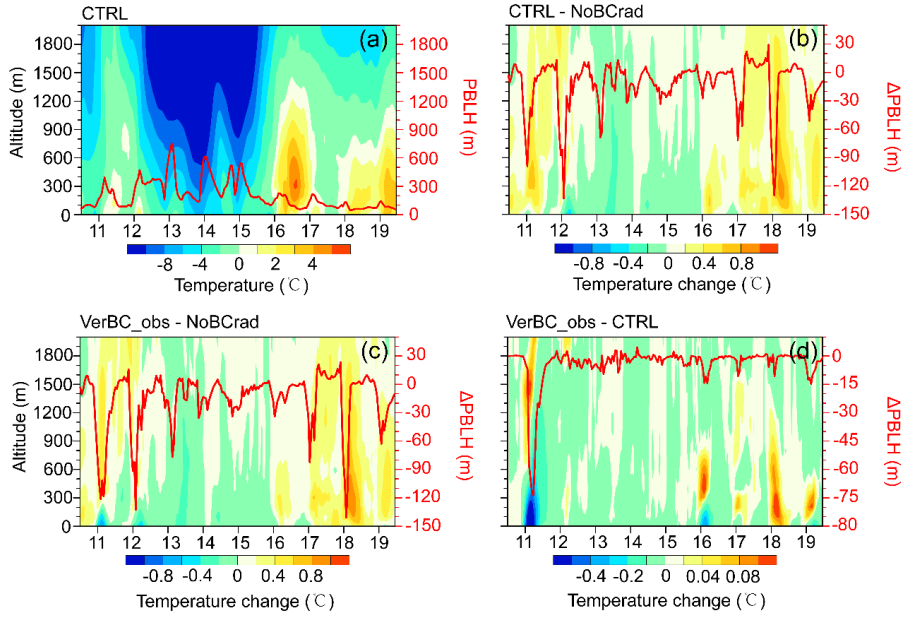

Figure 7. (a) Simulated hourly vertical profiles of temperature (contour) and PBLH (red solid line) over Beijing at local time (LT) from 11 December 2016 to 19 December 2016. (b-d) Time series of changes in vertical temperature (contour) and PBLH (ΔPBLH; red solid line) induced by BC DRE with original (b; CTRL minus NoBCrad) and modified vertical profiles (c; VerBC_obs minus NoBCrad), and the difference between the effects of modified and original BC profiles (d; VerBC_obs minus CTRL) over Beijing region from 11 December 2016 to 19 December 2016.

https://doi.org/10.5194/acp-2021-611
Preprint. Discussion started: 6 September 2021

Atmospheric Chemistry and Physics Discussions

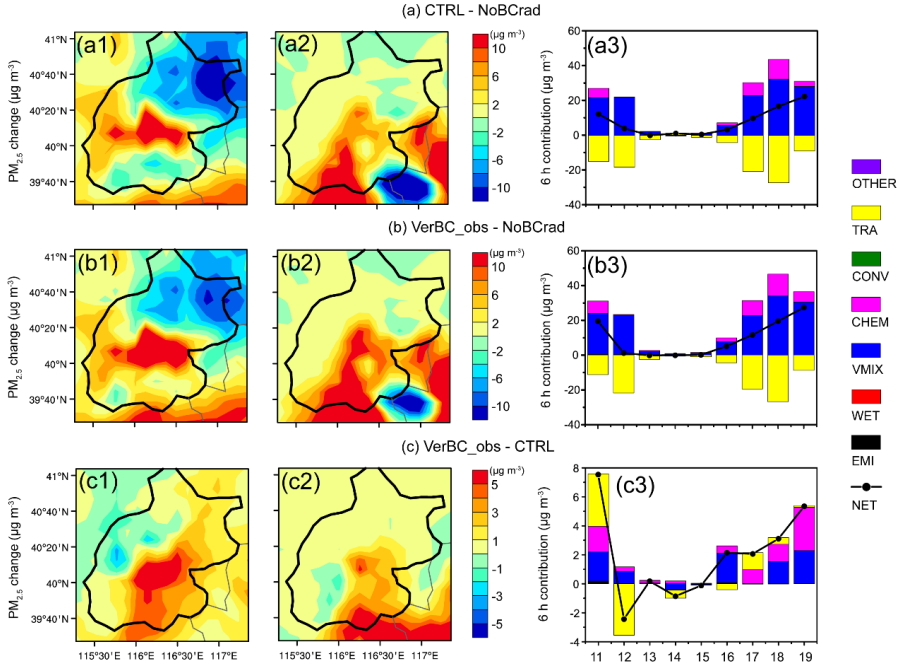

908

909 **Figure 8.** The spatial distribution of changes in near-surface $PM_{2.5}$ concentrations
910 induced by BC DRE with original (CTRL minus NoBCrad; a1 and a2) and modified
911 vertical profiles (VerBC_obs minus NoBCrad; b1 and b2), and the difference between
912 VerBC_obs and CTRL (VerBC_obs minus CTRL; c1 and c2) over Beijing averaged
913 over the period of 12:00 – 18:00 LT of the two haze events. a1-c1 represent the first
914 pollution event of 11-12 December 2016 and a2-c2 represent the second pollution event
915 of 16-19 December 2016. (a3-c3) The daily 6-h contributions of each physical/chemical
916 process (colored bars, each of which is calculated as the concentration at 18:00 minus
917 that at 12:00) to the change in $PM_{2.5}$ in Beijing from 11 December 2016 to 19 December
918 2016. The black dotted line represents the 6-h net contribution to $PM_{2.5}$ change by
919 summing over all processes.

920

https://doi.org/10.5194/acp-2021-611
Preprint. Discussion started: 6 September 2021

Atmospheric Chemistry and Physics Discussions

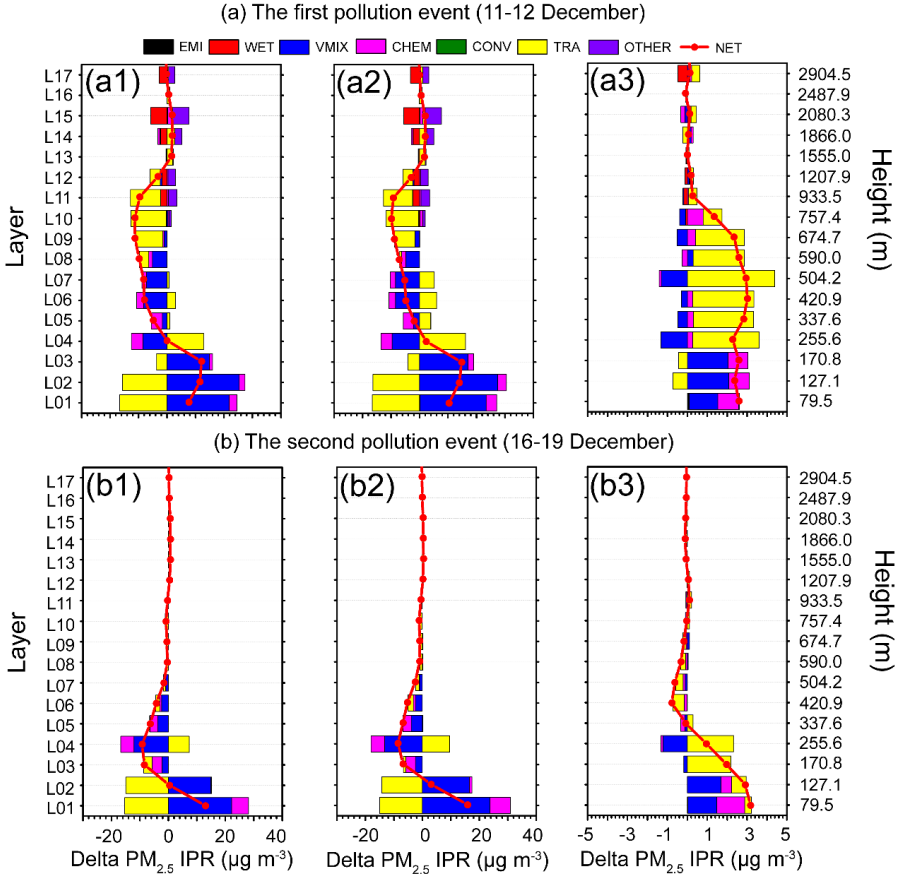

921

922 **Figure 9.** Vertical profiles of the 6-h contributions of physical/chemical processes
923 (colored bars; each is calculated as the concentration at 18:00 LT minus that at 12:00
924 LT) to the changes in $PM_{2.5}$ induced by BC DRE with original (CTRL minus
925 NoBCrad; a1 and b1) and modified vertical profiles (VerBC_obs minus NoBCrad; a2
926 and b2), and the difference between original and modified BC profiles (VerBC_obs
927 minus CTRL; a3 and b3) over Beijing. The red dotted lines represent the 6-h net
928 contributions to $PM_{2.5}$ changes by summing over all processes.

929

https://doi.org/10.5194/acp-2021-611
Preprint. Discussion started: 6 September 2021

Atmospheric Chemistry and Physics Discussions

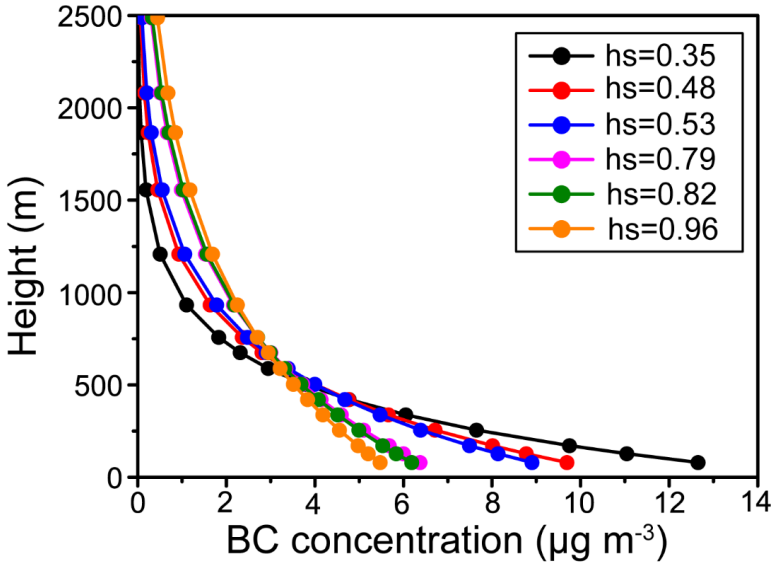

930

931 **Figure 10.** Vertical profiles of BC concentrations parameterized as six exponential

932 functions for 12 and 16-19 December 2016.

https://doi.org/10.5194/acp-2021-611
Preprint. Discussion started: 6 September 2021

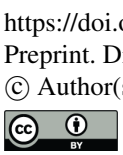

Atmospheric Chemistry and Physics Discussions

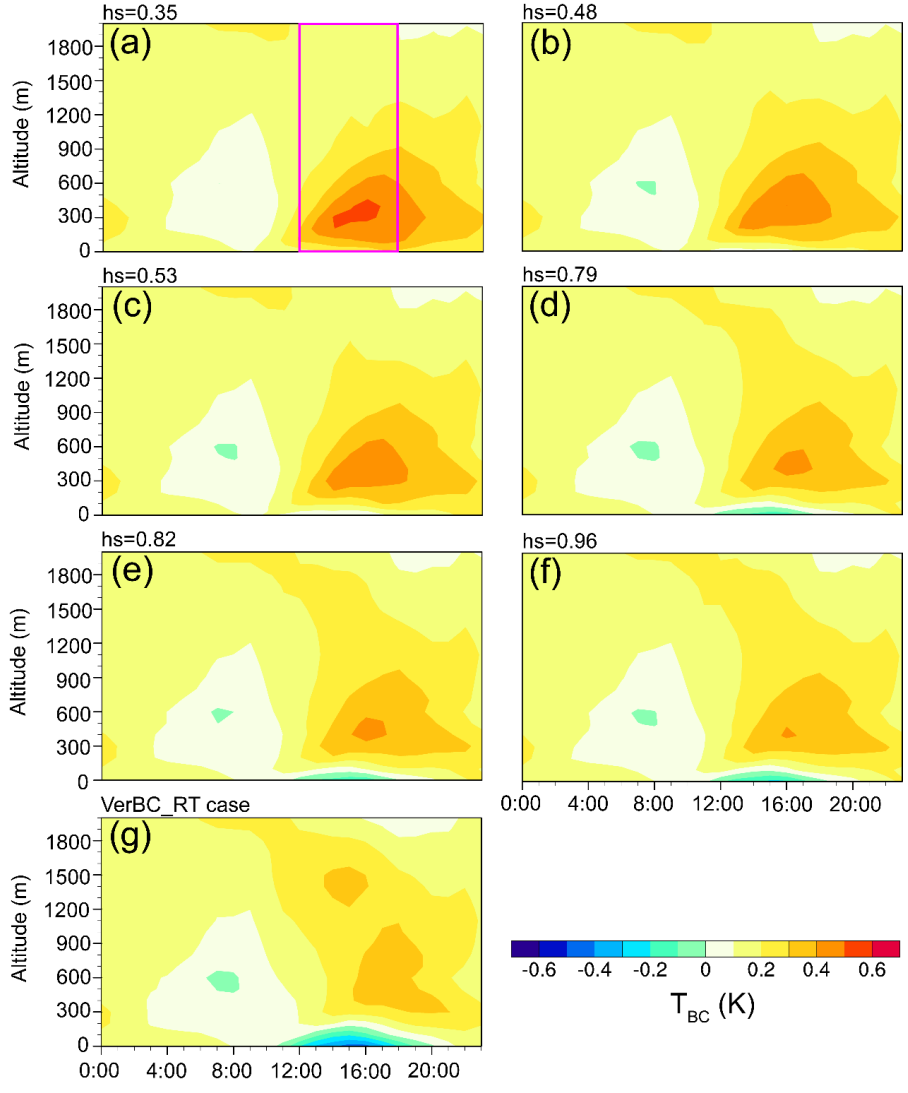

933

934 **Figure 11.** Time series of changes in vertical temperature induced by BC DRE with six
935 exponential functions (VerBC_hs1-6 minus NoBCrad) and one transport-dominated
936 vertical profile (VerBC_RT minus NoBCrad) averaged over 12 and 16-19 December
937 2016.

938

https://doi.org/10.5194/acp-2021-611
Preprint. Discussion started: 6 September 2021

Atmospheric Chemistry and Physics Discussions

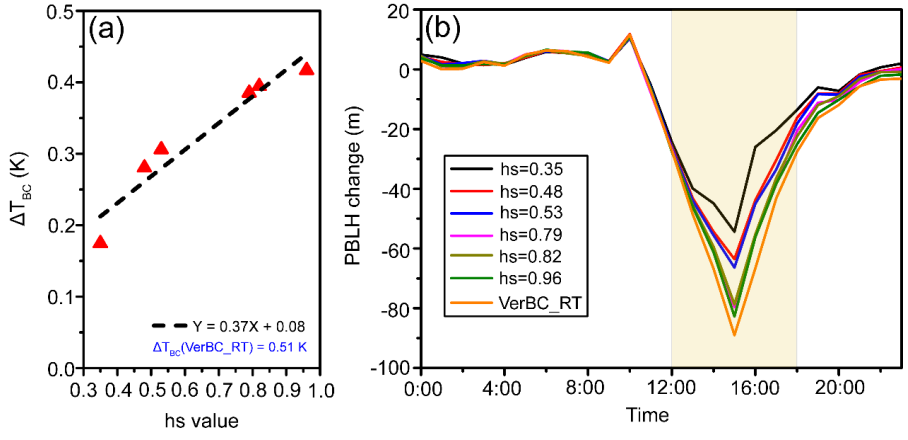

939

940 **Figure 12.** (a) Variation of ΔT_{BC} caused by BC DRE with increasing *hs* values averaged
941 12 and 16-19 December. The black dash line is the linear fit. (b) Time series of changes
942 in PBLH in Beijing caused by different BC vertical profiles averaged 12 and 16-19
943 December 2016.

944

https://doi.org/10.5194/acp-2021-611
Preprint. Discussion started: 6 September 2021

Atmospheric Chemistry and Physics Discussions

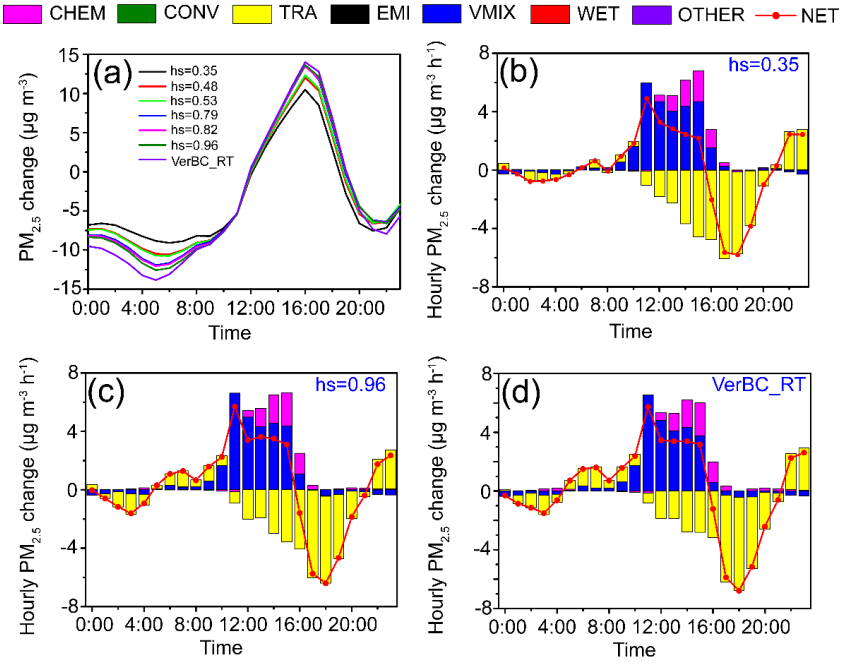

945

946 **Figure 13.** (a) Time series of the changes in surface-layer $PM_{2.5}$ in Beijing caused by
947 BC with six exponential functions (VerBC_hs1-6 minus NoBCrad) and one observed
948 transport-dominated vertical profile (VerBC_RT minus NoBCrad) averaged 12 and 16-
949 19 December 2016. (b-d) The hourly contributions of each physical/chemical process
950 to $PM_{2.5}$ changes caused by BC DRE with two exponential functions (*hs*=0.35 and 0.96)
951 and one transport-dominated vertical profile.

952